

# RSC Advances



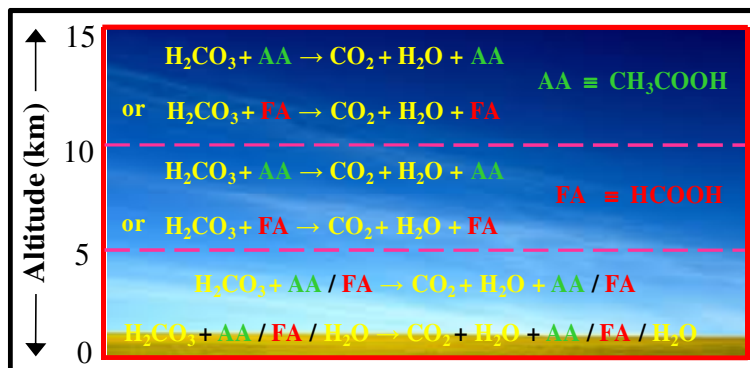
This is an *Accepted Manuscript*, which has been through the Royal Society of Chemistry peer review process and has been accepted for publication.

*Accepted Manuscripts* are published online shortly after acceptance, before technical editing, formatting and proof reading. Using this free service, authors can make their results available to the community, in citable form, before we publish the edited article. This *Accepted Manuscript* will be replaced by the edited, formatted and paginated article as soon as this is available.

You can find more information about *Accepted Manuscripts* in the [Information for Authors](#).

Please note that technical editing may introduce minor changes to the text and/or graphics, which may alter content. The journal's standard [Terms & Conditions](#) and the [Ethical guidelines](#) still apply. In no event shall the Royal Society of Chemistry be held responsible for any errors or omissions in this *Accepted Manuscript* or any consequences arising from the use of any information it contains.

## Graphical Abstract



Carbonic Acid Decomposition of Potential Atmospheric Significance

# **H<sub>2</sub>CO<sub>3</sub> → CO<sub>2</sub> + H<sub>2</sub>O Decomposition in Presence of H<sub>2</sub>O, HCOOH, CH<sub>3</sub>COOH, H<sub>2</sub>SO<sub>4</sub> and HO<sub>2</sub> Radical: Instability of the Gas-Phase H<sub>2</sub>CO<sub>3</sub> Molecule in Troposphere and Lower Stratosphere**

*Sourav Ghoshal and Montu K. Hazra \**

*Chemical Sciences Division, Saha Institute of Nuclear Physics, 1/AF Bidhannagar, Kolkata-700 064, India*

## **ABSTRACT**

To understand the stability of the gas-phase carbonic acid (H<sub>2</sub>CO<sub>3</sub>) molecule, especially, in the Earth's troposphere and lower stratosphere, here we report high levels of quantum chemistry calculations investigating the energetics for the H<sub>2</sub>CO<sub>3</sub> → CO<sub>2</sub> + H<sub>2</sub>O decomposition reaction via its shortest route in presence of one to three water (H<sub>2</sub>O) molecules as well as in presence of the formic acid (FA), acetic acid (AA), sulfuric acid (SA) and hydroperoxide (HO<sub>2</sub>) radical. The calculations have been performed at the MP2/aug-cc-pVDZ, MP2/aug-cc-pVTZ, MP2/6-311++G(3df,3pd) and CCSD(T)/aug-cc-pVTZ levels of theories. The comparison of the reaction rates including tunneling corrections according to the unsymmetrical Eckart potential barriers suggests that at 0 km altitude in the clean environments of the Earth's atmosphere, the gaseous H<sub>2</sub>CO<sub>3</sub> molecule becomes an unstable species in presence of the H<sub>2</sub>O monomer, dimer, FA and AA. This follows as the FA and AA assisted H<sub>2</sub>CO<sub>3</sub> → CO<sub>2</sub> + H<sub>2</sub>O decomposition reactions are effectively the near-barrierless processes and the reaction rates for the H<sub>2</sub>O monomer, dimer, FA and AA assisted H<sub>2</sub>CO<sub>3</sub> decomposition reactions are comparable within the factor of ~10. Similarly, at 0 km altitude in the polluted environments and also, in the 5 to 15 km altitude range, only the FA or AA assisted H<sub>2</sub>CO<sub>3</sub> decomposition is the dominant channel, especially, among all the pathways those have been considered here. It is seen from the CCSD(T)/aug-cc-pVTZ level predicted results that at the 5, 10, and 15 km altitudes of the Earth's atmosphere, the reaction rates for the FA assisted H<sub>2</sub>CO<sub>3</sub> decomposition depending upon the average concentrations of FA are respectively ~10<sup>2</sup>, 10<sup>4</sup> and 10<sup>6</sup> times higher than the reaction rates associated with the water monomer assisted H<sub>2</sub>CO<sub>3</sub> decomposition. Moreover, it is thought that the catalytic efficiencies of the FA, AA and SA upon the H<sub>2</sub>CO<sub>3</sub> → CO<sub>2</sub> + H<sub>2</sub>O decomposition reaction are similar from each other, nevertheless, the SA, because of its low concentration, does not play any significant role in the H<sub>2</sub>CO<sub>3</sub> → CO<sub>2</sub> + H<sub>2</sub>O decomposition reaction, especially, in the 0 to 15 km altitude range of the Earth's atmosphere.

\* Address correspondence to: [h.montu@saha.ac.in](mailto:h.montu@saha.ac.in)

## 1. Introduction

Carbonic acid ( $\text{H}_2\text{CO}_3$ ) has been considered as the molecule of profound astrophysical as well as environmental significance as both the  $\text{H}_2\text{O}$  and  $\text{CO}_2$  molecules coexist in various astrophysical environments such as ice grain mantles in interstellar medium and/or in outer space.<sup>1-33</sup> This molecule was long believed to be an unstable and elusive species as it decomposes rapidly into  $\text{CO}_2$  and  $\text{H}_2\text{O}$  molecules.<sup>1,34-35</sup> Indeed, it had also been believed in past that the isolated  $\text{H}_2\text{CO}_3$  molecule cannot exist in free state and consequently, the existence of isolated  $\text{H}_2\text{CO}_3$  molecule in the gas-phase was controversial for a long time.<sup>2</sup> In 1987, Terlouw et al.<sup>1</sup> first detected the free  $\text{H}_2\text{CO}_3$  molecule in the gas-phase from the thermolysis of the ammonium bicarbonate ( $\text{NH}_4\text{HCO}_3$ ) molecule via mass spectrometry and hence, thereafter, the evidence for the possible existence of the  $\text{H}_2\text{CO}_3$  molecule in the gas-phase was established. Subsequently, in the next two and half decades, the gaseous  $\text{H}_2\text{CO}_3$  molecule has also been characterized in the laboratory by means of its microwave<sup>3-4</sup> and infrared<sup>5-6,36</sup> spectra. Moreover, the  $\text{H}_2\text{CO}_3$  molecule has also been synthesized in various experimental conditions in the laboratory similar to those encountered in the extraterrestrial space.<sup>7-15,37</sup> It is worth noting here that the  $\text{H}_2\text{CO}_3$  molecule is believed to be present in cirrus clouds of the Earth's atmosphere, on Venus and Martian surfaces, as well as in Comets and the Galilean satellites.<sup>2,5-6,21,28-30</sup> As noted by Kohl et al.,<sup>28</sup> a comparison of some spectra on Mars with the IR spectrum of  $\beta\text{-H}_2\text{CO}_3$ , which is known to date as the *distinct* polymorph of  $\text{H}_2\text{CO}_3$ ,<sup>5-6,21,26-30,36</sup> suggests that the  $\beta\text{-H}_2\text{CO}_3$  is present on the Martian surface.<sup>20</sup>

Given that the  $\text{H}_2\text{CO}_3$  monomer has been detected in various experimental conditions in the laboratory similar to those encountered in the extraterrestrial space, it is surprising that this molecule has not been detected yet in the Earth's atmosphere or in outer space.<sup>2,6,15</sup> Indeed, we note what has already been emphasized by Huber et al.,<sup>2</sup> Bernard et al.<sup>6</sup> and Hudson et al.<sup>22</sup> that the detection of gas-phase  $\text{H}_2\text{CO}_3$  molecule in the Earth's troposphere and as well as in outer space has become very challenging for a new generation of scientists.<sup>2,5-6,22</sup> Recently, we have demonstrated that the primary mechanism for the

decomposition of  $\text{H}_2\text{CO}_3$  molecule into its constituents  $\text{CO}_2$  and  $\text{H}_2\text{O}$  molecules, especially at its source, where the vapor phase concentration of the  $\text{H}_2\text{CO}_3$  molecule reaches its highest level, is autocatalytic.<sup>38</sup> In other words, the  $\text{H}_2\text{CO}_3$  molecule decomposes in presence of another  $\text{H}_2\text{CO}_3$  molecule when the vapor phase concentration of  $\text{H}_2\text{CO}_3$  molecule reaches its highest level. However, this autocatalytic decomposition mechanism is not expected to be the primary decomposition mechanism in the Earth's atmosphere or in the surroundings away from the source points of  $\text{H}_2\text{CO}_3$ . This follows as the probability of bimolecular encounters between the two  $\text{H}_2\text{CO}_3$  molecules is expected to fall off significantly due to dilution of carbonic acid concentration resulting from the presence of other various species detected in the Earth's atmosphere or in the surroundings away from the source points of  $\text{H}_2\text{CO}_3$ . It is also worthwhile to note here that the results of recent experiment from the Loerting et al.<sup>33</sup> group suggest undeniably that in our atmosphere some solid  $\text{H}_2\text{CO}_3$  may be present in cirrus clouds or on mineral dust, as in the middle or upper troposphere the reaction between mineral dust particles containing  $\text{CaCO}_3$  and acids like  $\text{HCl}$  can produce solid  $\text{H}_2\text{CO}_3$  which remains intact at cold temperatures (210-260K) and under high relative humidity.<sup>6,33</sup> Also, as the wide range of temperature found in the troposphere matches with the range of temperature at which this solid  $\text{H}_2\text{CO}_3$  sublimates, the gaseous  $\text{H}_2\text{CO}_3$  molecules may indeed be present in the middle or upper troposphere via the sublimations of the solid  $\text{H}_2\text{CO}_3$ .<sup>6,33</sup> Moreover,  $\text{H}_2\text{CO}_3$  may also form in upper troposphere by the reaction of  $\text{CO}_2$  and  $\text{H}_2\text{O}$  in a water cluster.<sup>21</sup>

Therefore, in view of the fact that the detection of gas-phase  $\text{H}_2\text{CO}_3$  in the Earth's troposphere and in outer space is very challenging,<sup>2,5-6,22</sup> it is important to investigate the stability of the  $\text{H}_2\text{CO}_3$  molecule in presence of other various species detected in the Earth's atmosphere and outer space. It is also important to note here that the decomposition of  $\text{H}_2\text{CO}_3$  molecule into its constituents  $\text{CO}_2$  and  $\text{H}_2\text{O}$  molecules in presence of one to three water molecules has been studied earlier;<sup>39-41</sup> but not in the scenario of potential atmospheric relevance. Very recently, the carboxylic acids ( $\text{RCO}_2\text{H}$ ) assisted decomposition of the  $\text{H}_2\text{CO}_3$  molecule into its constituents  $\text{CO}_2$  and  $\text{H}_2\text{O}$  molecules has been studied by Kumar et al.<sup>42-43</sup> and

the primary focus of this work was to explore the instability of the gaseous  $\text{H}_2\text{CO}_3$  molecule in presence of carboxylic acids in comparison to the water monomer assisted  $\text{H}_2\text{CO}_3$  decomposition, especially, at the 0 km altitude of the Earth's atmosphere. However, as the gaseous  $\text{H}_2\text{CO}_3$  molecule is also believed to be present in cirrus clouds of the Earth's atmosphere or in the middle and/or upper troposphere of the Earth's atmosphere, it is also important to inquire the stability of the gaseous  $\text{H}_2\text{CO}_3$  molecule with respect to the concentrations of water and carboxylic acids present not only in the middle and/or upper troposphere but also in the lower stratosphere. It is to be noted here that the cirrus clouds in the Earth's atmosphere are typically observed in the upper troposphere and in lower stratosphere.<sup>44-45</sup>

Moreover, the shortest route for the gas-phase decomposition of the isolated  $\text{H}_2\text{CO}_3$  molecule into its constituents  $\text{CO}_2$  and  $\text{H}_2\text{O}$  molecules is the concerted mechanism that involves dehydroxylation of one particular OH functional group and a simultaneous dehydrogenation of other OH functional group among the two nonequivalent OH functional groups present in the *cis-trans* conformer of  $\text{H}_2\text{CO}_3$  molecule (Fig. 1A).<sup>39-41</sup> Note here that the *cis-trans* conformer of  $\text{H}_2\text{CO}_3$ , as shown in Fig. 1A, is the second most stable conformer of carbonic acid and it is the starting point for the decomposition of  $\text{H}_2\text{CO}_3$  molecule into its constituents  $\text{CO}_2$  and  $\text{H}_2\text{O}$  molecules (see below).<sup>38-41</sup> In addition, to visualize how the water ( $\text{H}_2\text{O}$ ), formic acid ( $\text{HC(O)OH} \equiv \text{FA}$ ) and the  $\text{H}_2\text{CO}_3$  molecule itself because of their simultaneous hydrogen donor and acceptor capabilities promote this hydrogen transfer process, we also present the shortest routes for the water, FA and  $\text{H}_2\text{CO}_3$  assisted decompositions of the  $\text{H}_2\text{CO}_3$  molecule in the same figure (Fig. 1B to 1D).<sup>38-40,42</sup> It is seen from the literature that the sulfuric acid ( $\text{H}_2\text{SO}_4 \equiv \text{SA}$ ) and hydroperoxide ( $\text{HO}_2$ ) radical, which have also been detected in the Earth's atmosphere, are also the effective catalysts like formic acid, especially, for the hydrogen transfer reactions via the O—H bond breaking and making processes within the doubly or multiply hydrogen-bonded interfaces.<sup>46-48</sup> Therefore, it is also important to investigate energetics and kinetics of the SA and  $\text{HO}_2$  radical assisted  $\text{H}_2\text{CO}_3$  decomposition reactions of potential atmospheric relevance, especially, with respect to the concentrations of these two species in the Earth's troposphere and lower stratosphere where the carbonic

acid is expected to exist. Thus, to understand the stability of the gaseous  $\text{H}_2\text{CO}_3$  molecule, especially, in the Earth's troposphere and lower stratosphere, here we focus upon the energetics of the potential energy diagrams as well as the simple relative kinetics for the decomposition of the  $\text{H}_2\text{CO}_3$  molecule into its constituents  $\text{CO}_2$  and  $\text{H}_2\text{O}$  molecules via its shortest route in presence of one to three water molecules as well as in presence of the formic acid (FA), acetic acid (AA), sulfuric acid (SA) and  $\text{HO}_2$  radical.

## 2. Computational Methods

Gaussian-09 suite of program with “**opt=tight**” convergence criteria has been used to carry out all the quantum chemistry calculations presented here.<sup>49</sup> Both the geometry optimizations and frequency calculations of the monomers and complexes have been performed using the second order Møller–Plesset (MP2) perturbation theory in conjunction with aug-cc-pVDZ, aug-cc-pVTZ and 6-311++G(3df,3pd) basis sets. It is worthwhile to note here that the geometry optimizations using the larger basis sets are required to reduce basis set superposition error (BSSE), even though full (100%) counterpoise corrections often underestimate binding energies of dimeric complexes.<sup>50-52</sup> Transition states (TS) have been located using the QST2/QST3 and OPT=TS routines as implemented in Gaussian-09 program. Furthermore, Intrinsic Reaction Coordinate (IRC) calculations were performed at the MP2/aug-cc-pVDZ level of theory to unambiguously verify that the transition states found connect with the desired reactants and products. In order to improve our estimates of the reaction energetics and reaction rate constants for the few selective reactions, we have also carried out single point energy calculations at the CCSD(T)/aug-cc-pVTZ level using the MP2/aug-cc-pVTZ level optimized geometries. Normal mode vibrational frequencies have been used to estimate the zero point vibration energy (ZPE) corrections for the reactants, products and TS. The computed total electronic energies ( $E_{\text{total}}$ ), ZPE corrected electronic energies [ $E_{\text{total}}(\text{ZPE})$ ] for the monomers, complexes and the transition states are given in Supplementary Table 1. In addition, normal mode vibrational frequency analyses have been performed for all the stationary points to verify that the stable minima have all positive

vibrational frequencies and that the transition states have only one imaginary frequency (see Supplementary Table-2).

### 3. Results and Discussion

It is seen from the high levels of theoretical calculations<sup>3-4,31-32,53-55</sup> that the H<sub>2</sub>CO<sub>3</sub> monomer has three conformers based on the different orientations of two OH functional groups present in the molecule and among these three conformers, the *cis-cis* [(*cc*)] and *cis-trans* [(*ct*)] conformers, as shown in the Fig. 2, are respectively the global minimum and the second most stable one.<sup>3-4</sup> Moreover, the (*ct*)-conformer, which is slightly energetically disfavored over the (*cc*)-conformer, is the starting point for the decomposition of H<sub>2</sub>CO<sub>3</sub> into its constituents CO<sub>2</sub> and H<sub>2</sub>O molecules,<sup>38-43</sup> as the direct decomposition of the isolated (*cc*)-H<sub>2</sub>CO<sub>3</sub> into its constituents CO<sub>2</sub> and H<sub>2</sub>O molecules is forbidden in the vapor phase. It is worthwhile to note here that though the direct decomposition of the isolated (*cc*)-H<sub>2</sub>CO<sub>3</sub> into its constituents CO<sub>2</sub> and H<sub>2</sub>O molecules is forbidden in vapor phase, nevertheless, our recent study<sup>55</sup> upon the energetics of the double hydrogen transfer in carbonic acid homodimers suggests that the interconversion of the (*cc*)-conformer to its (*ct*)-conformer [(*cc*)-H<sub>2</sub>CO<sub>3</sub> → (*ct*)-H<sub>2</sub>CO<sub>3</sub>] is also autocatalytic and potentially allowed, in particular, during the sublimation of pure H<sub>2</sub>CO<sub>3</sub> polymorphs at the cold temperatures. Therefore, taking the note that the (*ct*)-conformer of H<sub>2</sub>CO<sub>3</sub> is the starting point for the decomposition of the H<sub>2</sub>CO<sub>3</sub> into its constituents CO<sub>2</sub> and H<sub>2</sub>O molecules [(*ct*)-H<sub>2</sub>CO<sub>3</sub> → CO<sub>2</sub> + H<sub>2</sub>O ≡ H<sub>2</sub>CO<sub>3</sub> → CO<sub>2</sub> + H<sub>2</sub>O], we first investigate the energetics of potential energy diagrams for the H<sub>2</sub>CO<sub>3</sub> decomposition in presence of one to three water molecules with various mechanistic paths of potential atmospheric relevance. Second, to compare the energetics of all these water assisted H<sub>2</sub>CO<sub>3</sub> → CO<sub>2</sub> + H<sub>2</sub>O decompositions reactions, we investigate the energetics of the potential energy diagrams for the H<sub>2</sub>CO<sub>3</sub> decomposition in presence of the FA, AA, SA and HO<sub>2</sub> radical those have been detected or present in the Earth's atmosphere at the significant trace levels.<sup>56-75</sup>

#### 3A. H<sub>2</sub>CO<sub>3</sub> Decomposition in Presence of One to Three Water Molecules:

In Fig. 3, we present the MP2/aug-cc-pVTZ level calculated potential energy diagram for the direct decomposition of the isolated  $\text{H}_2\text{CO}_3$  molecule into its constituents  $\text{CO}_2$  and  $\text{H}_2\text{O}$  molecules [ $\text{H}_2\text{CO}_3 \rightarrow \text{CO}_2 + \text{H}_2\text{O}$ ]. The MP2/aug-cc-pVTZ level optimized geometries of the  $\text{H}_2\text{CO}_3$  reactant,  $\text{CO}_2 \cdots \text{H}_2\text{O}$  product complex and transition state (TS) have also been shown in the potential energy diagram. It is worthwhile to note here that the  $\text{H}_2\text{CO}_3$  reactant, which has been shown in the Fig. 3, is the (*ct*)-conformer of  $\text{H}_2\text{CO}_3$  and also, the (*ct*)-conformer of  $\text{H}_2\text{CO}_3$  is the starting point for the decomposition of the isolated  $\text{H}_2\text{CO}_3$  molecule into its constituents  $\text{CO}_2$  and  $\text{H}_2\text{O}$  molecules. From Fig. 3 and as noted above that the  $\text{H}_2\text{CO}_3 \rightarrow \text{CO}_2 + \text{H}_2\text{O}$  decomposition occurs via the transfer of a hydrogen atom from a particular OH functional group to the oxygen atom of the other nonequivalent OH functional group present within the  $\text{H}_2\text{CO}_3$  reactant (Fig. 1A). Note that the two OH functional groups present in the  $\text{H}_2\text{CO}_3$  reactant are nonequivalent as their orientation are different with respect to the orientation of the C=O functional group present within the  $\text{H}_2\text{CO}_3$  reactant. For comparison, in the same figure, we also present the potential energy diagram for the water monomer ( $\text{H}_2\text{O}$ ) assisted  $\text{H}_2\text{CO}_3 \rightarrow \text{CO}_2 + \text{H}_2\text{O}$  decomposition reaction. The MP2/aug-cc-pVTZ level optimized geometries of the entrance channel pre-reactive  $\text{H}_2\text{CO}_3 \cdots \text{H}_2\text{O}$  complex (**RC-I**), exit channel  $\text{CO}_2 \cdots \text{H}_2\text{O} \cdots \text{H}_2\text{O}$  product complex (**PC-I**) and the transition state (**TS-I**) associated with the  $\text{H}_2\text{O}$ -assisted  $\text{H}_2\text{CO}_3$  decomposition reaction have also been shown in the Fig. 3. As expected, the water molecule because of its simultaneous hydrogen donor and acceptor capability promotes the above mentioned hydrogen transfer process (Fig. 1A). At the MP2/aug-cc-pVTZ level of calculations, it is seen that the effective barrier, defined as the difference between the zero point vibrational energy (ZPE) corrected energy of the transition state and the total energy of the isolated starting reactants in terms of bimolecular encounters, in case of the  $\text{H}_2\text{O}$ -assisted decomposition reaction is  $\sim 13.5$  kcal/mol and this value is approximately three times lower than the barrier height associated with the naked  $\text{H}_2\text{CO}_3 \rightarrow \text{CO}_2 + \text{H}_2\text{O}$  decomposition reaction. The predicted barrier height for the naked  $\text{H}_2\text{CO}_3 \rightarrow \text{CO}_2 + \text{H}_2\text{O}$  unimolecular decomposition reaction at the MP2/aug-

cc-pVTZ level including ZPE correction is  $\sim 36.8$  kcal/mol. The calculated binding energies of the various complexes as well as the barrier heights for the rate limiting unimolecular decomposition steps, as discussed in this article, have been given in Table 1 and 2. From Table 1 and 2, it is seen that the predicted binding energies as well as barrier heights at the MP2 level of calculations are consistent for the three different basis sets used.

The  $\text{H}_2\text{CO}_3 \rightarrow \text{CO}_2 + \text{H}_2\text{O}$  decomposition reaction in presence of two water molecules have been considered to occur mainly in two different reaction pathways. First, the reaction pathway where the water dimer  $[(\text{H}_2\text{O})_2]$  assists actively to facilitate the above mentioned hydrogen transfer process required for the decomposition of  $\text{H}_2\text{CO}_3$ . It is worthwhile to note here that the  $(\text{H}_2\text{O})_2$  is present in the Earth's atmosphere at the significant trace levels.<sup>47,76</sup> Second, the reaction pathway where the second water molecule among the two water molecules stabilizes either actively or passively the pre-reactive  $\text{H}_2\text{CO}_3 \cdots \text{H}_2\text{O}$  complex (**RC-I**) and/or the **TS-I**, which have been located for the  $\text{H}_2\text{O}$ -assisted  $\text{H}_2\text{CO}_3$  decomposition reaction. It is to be noted here that this second pathway, where the second water molecule among the two water molecules participates the  $\text{H}_2\text{CO}_3$  decomposition either actively or passively, is based on the roles of the second water molecule if it assists either actively or passively the intermolecular hydrogen transfer process required for the  $\text{H}_2\text{O}$ -assisted  $\text{H}_2\text{CO}_3$  decomposition, as described earlier (Fig. 1B). Through these two main pathways, a total of three optimized geometries for the entrance channel  $\text{H}_2\text{CO}_3 \cdots \text{H}_2\text{O} \cdots \text{H}_2\text{O}$  pre-reactive complexes (**RC-II, III and IV**), as shown in Fig. 4, were located. In Fig. 4, we have also shown the optimized geometries of the corresponding transition states (**TS-II, III and IV**) and the exit channel  $\text{CO}_2 \cdots \text{H}_2\text{O} \cdots \text{H}_2\text{O} \cdots \text{H}_2\text{O}$  product complexes (**PC-II, III and IV**) associated with these three different  $\text{H}_2\text{CO}_3 \cdots \text{H}_2\text{O} \cdots \text{H}_2\text{O}$  pre-reactive complexes (**RC-II, III and IV**). The MP2/aug-cc-pVTZ level calculated potential energy diagrams associated with these three different pre-reactive complexes (**RC-II, III and IV**) including their respective ZPE corrections have been shown in Fig. 5. Note here that the **RC-II** is common pre-reactive complex in case of pathways where the  $(\text{H}_2\text{O})_2$  participates the  $\text{H}_2\text{CO}_3$  decomposition reaction actively and where the second water

molecule among the two water molecules stabilizes actively the pre-reactive  $\text{H}_2\text{CO}_3\cdots\text{H}_2\text{O}$  complex (**RC-I**) located for the  $\text{H}_2\text{O}$ -assisted decomposition reaction. Indeed, from our relative rate analysis (see below), we show that both channels are of near equal possibilities to occur in the Earth's atmosphere. Moreover, it is also worthwhile to note here that the  $\text{H}_2\text{CO}_3\cdots\text{H}_2\text{O}\cdots\text{H}_2\text{O}$  pre-reactive complex can also be formed through ternary collisions involving  $\text{H}_2\text{CO}_3$  and two  $\text{H}_2\text{O}$  molecules, nevertheless, the probability of this three-body collision occurring is expected to be relatively low in the Earth's atmosphere. From Fig. 5, it is seen that the most dominant channel according to the lowest and effective potential energy barrier height, as defined above, is the pathway where the  $\text{H}_2\text{CO}_3$  molecule hits the water dimer  $[(\text{H}_2\text{O})_2]$  directly and when the  $(\text{H}_2\text{O})_2$  assist the hydrogen transfer process actively. At the MP2/aug-cc-pVTZ level of calculation including ZPE corrections, the effective barrier height for this  $(\text{H}_2\text{O})_2$ -assisted decomposition pathway is only  $\sim 5.6$  kcal/mol. This value is more than two times lower than the barrier height associated with the  $\text{H}_2\text{O}$ -assisted  $\text{H}_2\text{CO}_3$  decomposition pathway. As mentioned above, the MP2/aug-cc-pVTZ level predicted effective barrier height for the  $\text{H}_2\text{O}$ -assisted  $\text{H}_2\text{CO}_3$  decomposition reaction is  $\sim 13.5$  kcal/mol. Moreover, the comparison of the potential energy profiles for the  $\text{H}_2\text{O}$  and  $(\text{H}_2\text{O})_2$  assisted decomposition reactions suggest that the successive addition of water molecules in the decomposition mechanism is not counterproductive when only the energetics of the potential energy diagrams are considered. Therefore, and next, we focus upon the  $\text{H}_2\text{CO}_3$  decomposition in presence of three water molecules with a variety of possible bimolecular encounters those are expected to be relevant in the Earth's atmosphere.

The  $\text{H}_2\text{CO}_3 \rightarrow \text{CO}_2 + \text{H}_2\text{O}$  decomposition reaction in presence of three water molecules can be considered as the participation of the third water molecule into all the reaction pathways those have been considered above in case of the two water molecules assisted  $\text{H}_2\text{CO}_3 \rightarrow \text{CO}_2 + \text{H}_2\text{O}$  decomposition reactions. In other words, and like before, these are the reaction pathways where the third water molecule among the three water molecules stabilizes either actively or passively the pre-reactive

$\text{H}_2\text{CO}_3 \cdots \text{H}_2\text{O} \cdots \text{H}_2\text{O}$  complexes (**RC-II, III and IV**) or the transition states (**TS-II, III and IV**) obtained above for the two water molecules assisted  $\text{H}_2\text{CO}_3$  decomposition reactions. Moreover, the water trimer  $[(\text{H}_2\text{O})_3]$ , which is also expected to be present in the Earth's atmosphere at the significant trace levels,<sup>76</sup> can assist the  $\text{H}_2\text{CO}_3 \rightarrow \text{CO}_2 + \text{H}_2\text{O}$  decomposition with the pathways where either the only one or two water subunits among the three water subunits present in the water trimer  $[(\text{H}_2\text{O})_3]$  participate actively. It is worthwhile to note here that unlike the optimized structure of the water dimer  $[(\text{H}_2\text{O})_2]$ , which is the single hydrogen-bonded (H-bonded) open complex, the water trimer  $[(\text{H}_2\text{O})_3]$  is the triple H-bonded cyclic complex.<sup>76</sup> Therefore, and overall, we note that there are numerous bimolecular encounters with respect to the  $\text{H}_2\text{CO}_3 + (\text{H}_2\text{O})_3$ ,  $\text{H}_2\text{CO}_3 \cdots \text{H}_2\text{O} + (\text{H}_2\text{O})_2$  and  $\text{H}_2\text{CO}_3 \cdots \text{H}_2\text{O} \cdots \text{H}_2\text{O} + \text{H}_2\text{O}$  reactant channels, which may result in the decompositions of  $\text{H}_2\text{CO}_3$  molecule into its constituents  $\text{CO}_2$  and  $\text{H}_2\text{O}$  molecules. Having rationalized all these numerous bimolecular encounters, we locate various geometries of the  $\text{H}_2\text{CO}_3 \cdots \text{H}_2\text{O} \cdots \text{H}_2\text{O} \cdots \text{H}_2\text{O}$  pre-reactive complexes. However, subsequent location of the transition states and IRC calculations suggest that many of them are irrelevant, as the IRC calculations of the transition states do not connect with many of the desired pre-reactive and exit-channel product complexes in terms of the shortest decomposition route as we have discussed above. Finally, in Fig 6, we present five different pre-reactive  $\text{H}_2\text{CO}_3 \cdots \text{H}_2\text{O} \cdots \text{H}_2\text{O} \cdots \text{H}_2\text{O}$  complexes (**RC-V, VI, VII, VIII and IX**) and their corresponding five different transition states (**TS-V, VI, VII, VIII and IX**) as well as their five exit channel  $\text{CO}_2 \cdots \text{H}_2\text{O} \cdots \text{H}_2\text{O} \cdots \text{H}_2\text{O} \cdots \text{H}_2\text{O}$  product complexes (**PC-V, VI, VII, VIII and IX**), which are connected via the IRC calculations. In Fig. 7, we present five different potential energy diagrams associated with the five different pre-reactive  $\text{H}_2\text{CO}_3 \cdots \text{H}_2\text{O} \cdots \text{H}_2\text{O} \cdots \text{H}_2\text{O}$  complexes (**RC-V, VI, VII, VIII and IX**). From Fig. 7, we first point out that for the bimolecular encounters between  $\text{H}_2\text{CO}_3$  and  $(\text{H}_2\text{O})_3$  reactants with the pathway where the only one water subunit among the three water subunits present in the water trimer  $[(\text{H}_2\text{O})_3]$  participate actively or for the decomposition pathway associated with the **RC-IX**, the effective barrier is 10.7 kcal/mol. This value is approximately two times higher than the effective barrier for the  $(\text{H}_2\text{O})_2$ -assisted  $\text{H}_2\text{CO}_3$  decomposition path. As mentioned above, the

effective barrier height for the  $(\text{H}_2\text{O})_2$ -assisted  $\text{H}_2\text{CO}_3$  decomposition path is  $\sim 5.6$  kcal/mol. Therefore, as the atmospheric concentration of the  $(\text{H}_2\text{O})_3$  is substantially lower than the concentration of the  $(\text{H}_2\text{O})_2$ ,<sup>76</sup> we find that this channel is not important with respect to the main focus of this article and hence, we ignore this channel straightway for further discussion from here onwards. Second, the most effective pathways according to the lowest and effective potential energy barriers are the bimolecular encounters between  $\text{H}_2\text{CO}_3 \cdots \text{H}_2\text{O}$  and  $(\text{H}_2\text{O})_2$  those result in the **RC-VI**, **VII** and **VIII**. This is because in these three pathways, the MP2/aug-cc-pVTZ level predicted effective barrier heights including ZPE correction, as defined above, are respectively and only  $\sim 3$ , 3.4 and  $\sim 3.6$  kcal/mol. These values are on an average  $\sim 1.7$  times lower than the barrier height associated with the  $(\text{H}_2\text{O})_2$ -assisted  $\text{H}_2\text{CO}_3$  decomposition pathway, as mentioned above. Therefore, and particularly, these three channels in the case of three water molecules assisted  $\text{H}_2\text{CO}_3$  decompositions are expected to have similar impacts from each other and also, expected to be more important in comparison to all the pathways those have been considered above for the water monomer and two water molecules assisted  $\text{H}_2\text{CO}_3$  decompositions. However, below we show from the relative reaction rate analysis with atmospheric concentrations of the  $\text{H}_2\text{O}$  monomer and dimer that among these three channels, the two channels, which are associated with the **RC-VII** and **VIII**, are actually less important in comparison to the  $\text{H}_2\text{O}$ ,  $(\text{H}_2\text{O})_2$ , formic acid (FA) and acetic acid (AA) assisted  $\text{H}_2\text{CO}_3 \rightarrow \text{CO}_2 + \text{H}_2\text{O}$  decomposition reactions.

### 3B. $\text{H}_2\text{CO}_3$ Decomposition in Presence of FA, AA, SA and $\text{HO}_2$ Radical:

In this section, we explore the reaction energetics for the  $\text{H}_2\text{CO}_3$  decomposition in presence of the formic acid (FA), acetic acid (AA), sulfuric acid (SA) and hydroperoxy ( $\text{HO}_2$ ) radical. These species are not only present at the significant trace levels in the Earth's atmosphere<sup>56-75</sup> but also known as the effective catalysts in case of the hydrogen transfer reactions in the doubly or multiply hydrogen-bonded interfaces via the O—H bond breaking and making process.<sup>46-48,77-83</sup> Like before, for the FA, AA, SA and  $\text{HO}_2$  radical assisted  $\text{H}_2\text{CO}_3$  decomposition reactions, the MP2/aug-cc-pVTZ level optimized geometries of transition states (**TS-X**, **XI**, **XII** and **XIII**) and their IRC verified pre-reactive complexes

(**RC-X, XI, XII and XIII**) and the exit channel product complexes (**PC-X, XI, XII and XIII**) have been shown in Fig. 8. In Fig. 9, we present the MP2/aug-cc-pVTZ level calculated potential energy profiles for these FA, AA, SA and HO<sub>2</sub> radical assisted H<sub>2</sub>CO<sub>3</sub> → CO<sub>2</sub> + H<sub>2</sub>O decomposition reactions. From Fig. 9, it is seen that the effective barriers, as defined before, for these FA, AA, SA and HO<sub>2</sub> assisted H<sub>2</sub>CO<sub>3</sub> decomposition reactions are negligible or very small with the transition states being at either slightly higher or lower energies with respect to the total energies of the isolated starting bimolecular reactants. Therefore, the catalytic efficiencies of FA, AA, SA and HO<sub>2</sub> radical upon the H<sub>2</sub>CO<sub>3</sub> → CO<sub>2</sub> + H<sub>2</sub>O decomposition reaction are more or less equal from each other, especially, at the MP2 level of theory. Moreover, the effective barriers for these decomposition reactions are similar to those we find in case of the two autocatalytic H<sub>2</sub>CO<sub>3</sub> → CO<sub>2</sub> + H<sub>2</sub>O decomposition reactions as reported by us very recently with respect to the two most stable conformers of carbonic acid.<sup>38</sup> Note that at the MP2/aug-cc-pVTZ level of calculations, the effective barriers for the two autocatalytic H<sub>2</sub>CO<sub>3</sub> decomposition reactions are respectively ~0.2 and ~1.7 kcal/mol with the transition states being at lower energies.<sup>38</sup> Therefore, the above results and especially the energetics of the potential energy diagrams for the FA and AA assisted H<sub>2</sub>CO<sub>3</sub> decompositions are the expected one, as these two carboxylic acids promote the H<sub>2</sub>CO<sub>3</sub> decomposition by their hydrogen donor (O—H) and hydrogen acceptor (C=O) functional groups in a similar way to that carbonic acid does in case of its autocatalytic decomposition (Fig. 1). Note here that the primary mechanism for the decomposition of H<sub>2</sub>CO<sub>3</sub> molecule into its constituents CO<sub>2</sub> and H<sub>2</sub>O molecules, especially at its source where the vapor phase concentration of the H<sub>2</sub>CO<sub>3</sub> molecule reaches its highest level, is autocatalytic<sup>38</sup> and this is based upon the experimental observation that the sublimation of pure H<sub>2</sub>CO<sub>3</sub> polymorphs results in the decomposition of H<sub>2</sub>CO<sub>3</sub> molecule into its constituents CO<sub>2</sub> and H<sub>2</sub>O in the water restricted environment.<sup>5-6</sup> Further detail analysis of the potential energy profiles, as presented in the Fig. 9, suggest that the most effective catalysts are the AA and SA when only the effective barriers of the potential energy profiles are considered. However, below we specifically show that the SA-assisted H<sub>2</sub>CO<sub>3</sub> → CO<sub>2</sub> + H<sub>2</sub>O decomposition reaction has not any

significant role in comparison to what we find in the cases of  $\text{H}_2\text{O}$ ,  $(\text{H}_2\text{O})_2$ , FA and AA assisted  $\text{H}_2\text{CO}_3 \rightarrow \text{CO}_2 + \text{H}_2\text{O}$  decomposition reactions, especially, in the Earth's troposphere and lower stratosphere. Thus, and finally, given that the FA, AA, SA and  $\text{HO}_2$  radical assisted  $\text{H}_2\text{CO}_3$  decompositions are effectively near-barrierless reactions and the catalytic efficiencies of FA, AA, SA and  $\text{HO}_2$  radical upon the  $\text{H}_2\text{CO}_3$  decomposition reaction are more or less equal from each other, we next explore the potential roles of all these pathways towards an understanding of the atmospheric instability of the gas-phase  $\text{H}_2\text{CO}_3$  molecule up to 15 km altitude from the Earth's surface. It is to be noted here that the carbonic acid is expected to be present in the Earth's troposphere and lower stratosphere.

### 3C. Relative Rates and Atmospheric Implications of the Above Results:

It has been mentioned earlier that the carbonic acid has not been detected yet in the Earth's atmosphere or at outer space either in the solid or in the gas-phase. Therefore, as the concentration of carbonic acid is not known in the Earth's atmosphere, we point out that the relative rate analysis is only the method by which one can explore the relative impacts of the various species upon the  $\text{H}_2\text{CO}_3 \rightarrow \text{CO}_2 + \text{H}_2\text{O}$  decomposition reaction in the Earth's atmosphere. It is worthwhile to note that in order to assess the impacts of various pathways discussed above, it is necessary to compare reaction rates rather than reaction rate constants. This follows as the various catalytic species may have similar catalytic efficiencies upon a reaction of potential atmospheric relevance but they may not have similar concentrations in the Earth's atmosphere. We also point out here that it is not the goal of the present work to calculate absolute rates but to only examine relative rates associated with reagent energetics computed at the same level of theory. The rate constants for various pathways, as discussed here, have been calculated by the conventional transition state theory (TST) including tunneling correction according to the unsymmetrical Eckart potential barriers.<sup>84-91</sup> The calculated rate constants for various pathways and the atmospheric concentrations of the water monomer, dimer, FA, AA, SA and  $\text{HO}_2$  radical have been tabulated in the Supplementary Information. Also, the computational methodology and equations used to estimate the reaction rates of various pathways with respect to rate of the water

monomer ( $\text{H}_2\text{O}$ ) assisted  $\text{H}_2\text{CO}_3 \rightarrow \text{CO}_2 + \text{H}_2\text{O}$  decomposition reaction have been given in detail in the Supplementary Information. Here we only provide and focus upon the final results of relative rates for all the decomposition pathways by taking the  $\text{H}_2\text{O}$ -assisted  $\text{H}_2\text{CO}_3$  decomposition reaction as the reference. The relative rates for all the decomposition pathways have been given in the Table 3 and 4. In table 3 and 4, the reaction rates ( $v_{\text{I}}$  to  $v_{\text{XIII}}$ ) for the various reaction pathways have been labeled according to the various pre-reactive complexes (**RC**). For example, the  $\text{H}_2\text{CO}_3$  decomposition reaction associated with the '**RC-I**' is corresponding to the reaction path '**R-I**' and the reaction rate ' $v_{\text{I}}$ '. Similarly, the  $\text{H}_2\text{CO}_3$  decomposition reaction associated with the **RC-XIII** is corresponding to the reaction path '**R-XIII**' and reaction rate ' $v_{\text{XIII}}$ '.

In order to keep the discussion simple here, we first discuss only the MP2/aug-cc-pVTZ level predicted relative rates at 0 km altitude of the Earth's environment for all the  $\text{H}_2\text{CO}_3$  decomposition pathways those have been considered in presence of one to three water molecules. From the data presented in Table 3, it is seen that the most predominant channel is the  $\text{H}_2\text{O}$ -assisted  $\text{H}_2\text{CO}_3$  decomposition reaction; even though the effective barrier height for this channel is substantially higher than the effective barrier heights associated with all the pathways considered for the two and three water molecules assisted  $\text{H}_2\text{CO}_3$  decomposition reactions. Moreover, the reaction rates for two and three water molecules assisted decomposition reactions, especially, those are associated with the **RC-II, III, V and VI**, are comparable with the rate calculated for the  $\text{H}_2\text{O}$ -assisted  $\text{H}_2\text{CO}_3$  decomposition reaction within the factor 10. Therefore, according to the MP2/aug-cc-pVTZ level of calculations, and if we consider the  $\text{H}_2\text{CO}_3 \rightarrow \text{CO}_2 + \text{H}_2\text{O}$  decomposition reaction in presence of water molecules only, it is thought that the  $\text{H}_2\text{O}$ -assisted  $\text{H}_2\text{CO}_3$  decomposition is the most predominant channel, nevertheless, the decomposition of  $\text{H}_2\text{CO}_3$  in presence of the two and three water molecules can not be ignored completely. Indeed, below we show that at the 0 km altitude in clean environment of the Earth's atmosphere, especially, the

$\text{H}_2\text{O}$  and  $(\text{H}_2\text{O})_2$  assisted  $\text{H}_2\text{CO}_3$  decomposition are more or less equally important with the FA and AA assisted  $\text{H}_2\text{CO}_3$  decomposition reactions.

It has been mentioned before that we have also carried out single point energy calculations at the CCSD(T)/aug-cc-pVTZ level using the MP2/aug-cc-pVTZ level optimized geometries for the few selective reactions to improve our estimates regarding the reaction energetics as well as the corresponding reaction rate constants. To compare the  $\text{H}_2\text{O}$  and  $(\text{H}_2\text{O})_2$  assisted  $\text{H}_2\text{CO}_3$  decompositions with the FA, AA, SA and  $\text{HO}_2$  radical assisted  $\text{H}_2\text{CO}_3$  decompositions on equal footing, the CCSD(T)/aug-cc-pVTZ level of calculations have been performed for the  $\text{H}_2\text{O}$ ,  $(\text{H}_2\text{O})_2$ , FA, AA, SA and  $\text{HO}_2$  radical assisted  $\text{H}_2\text{CO}_3$  decomposition reactions. The CCSD(T)/aug-cc-pVTZ level estimated binding energies of pre-reactive and exit channel complexes as well as the effective barrier heights associated with the  $\text{H}_2\text{O}$ ,  $(\text{H}_2\text{O})_2$ , FA, AA, SA and  $\text{HO}_2$  radical assisted decomposition reactions have been given in Table 1 and 2. The CCSD(T)/aug-cc-pVTZ level predicted rate constants for the decompositions of the  $\text{H}_2\text{CO}_3$  molecule in presence of  $\text{H}_2\text{O}$ ,  $(\text{H}_2\text{O})_2$ , FA, AA, SA and  $\text{HO}_2$  radical have been given in the Supplementary Information and the calculated relative rates at the same level of theory for these reactions with respect to the  $\text{H}_2\text{O}$ -assisted  $\text{H}_2\text{CO}_3$  decomposition have been given in the Table 3 and 4. From the results at the CCSD(T)/aug-cc-pVTZ level of calculations, it is seen that the effective barriers, as defined above, are sensitive to some extents to the levels of calculations used, especially and specifically, in the case of  $\text{HO}_2$ -assisted  $\text{H}_2\text{CO}_3$  decomposition reaction. For the  $\text{HO}_2$ -assisted decomposition, it is thought that there is a substantial discrepancy between the MP2/aug-cc-pVTZ and CCSD(T)/aug-cc-pVTZ levels predicted barrier heights and/or reaction rates, nevertheless, the results predicted at the CCSD(T)/aug-cc-pVTZ level offer similar conclusion with respect to that we find from the results predicted at the MP2/aug-cc-pVTZ level of theories. In both the levels of calculations, we find that the  $\text{HO}_2$ -assisted  $\text{H}_2\text{CO}_3$  decomposition does not play any significant role in the Earth's troposphere and lower stratosphere. This follows as the concentration of the  $\text{HO}_2$  radical is substantially lower than the concentration of FA in the 0 to 15 km altitude of the Earth's atmosphere (see

Supplementary Information). The comparison of the CCSD(T)/aug-cc-pVTZ level predicted relative rates for the H<sub>2</sub>O, (H<sub>2</sub>O)<sub>2</sub>, FA, AA, and SA assisted H<sub>2</sub>CO<sub>3</sub> decomposition reactions, as presented in the Table 3 and 4, suggest that the AA-assisted decomposition reaction is the predominant channel at 0 km altitude and the rate for the AA-assisted decomposition reaction is respectively ~13 and 41 times higher than the reaction rates obtained for the FA and water monomer assisted H<sub>2</sub>CO<sub>3</sub> decompositions. It is worthwhile to note here the this prediction is based on the results obtained at the CCSD(T)/aug-cc-pVTZ level of theory. At the MP2/aug-cc-pVTZ level of theory, the rate for the AA assisted H<sub>2</sub>CO<sub>3</sub> decomposition reaction is ~8 times higher than the similar rates obtained for both the FA and H<sub>2</sub>O assisted H<sub>2</sub>CO<sub>3</sub> decompositions. Furthermore, as has been pointed out in the Supplementary Information that the average concentration of the FA or AA ( $6.1 \times 10^{10}$  molecules/cm<sup>3</sup>  $\equiv$  3.87 ppbv) at 0 km altitude, which we have taken into account in our rate calculations, is approximately and at least 4 to 5 times higher than the measured concentrations of the FA or AA present in the clean environment of the Earth's atmosphere.<sup>57</sup> This follows as the clean and polluted environments of the Earth's atmosphere are defined according to the typical surface mixing ratios<sup>74</sup> of the FA or AA respectively less than 1ppbv and more than 10 ppbv.<sup>57</sup> Therefore, in polluted areas, where the mixing ratios of FA and AA reach ~10 ppbv ( $\sim 1.6 \times 10^{11}$  molecules/cm<sup>3</sup>) or above,<sup>57</sup> the RCO<sub>2</sub>H-assisted H<sub>2</sub>CO<sub>3</sub> decomposition is only the dominant channel (RCO<sub>2</sub>H  $\equiv$  carboxylic acids). However, if we consider the measured concentrations of the FA and AA in the clean environment<sup>57</sup> or when the FA and AA mixing ratios in the rural, urban, semi urban and forest areas,<sup>56-58,62-69</sup> are less than 1 ppbv ( $\sim 1.6 \times 10^{10}$  molecules/cm<sup>3</sup>), the H<sub>2</sub>O-assisted H<sub>2</sub>CO<sub>3</sub> decomposition get its impact in between the AA and FA assisted H<sub>2</sub>CO<sub>3</sub> decomposition reactions. For example, when we consider the CCSD(T)/aug-cc-pVTZ predicted rates and the mixing ratio ~0.75 ppbv ( $\sim 1.2 \times 10^{10}$  molecules/cm<sup>3</sup>) for both the FA and AA, the reaction rate for the H<sub>2</sub>O-assisted decomposition reaction is respectively 2 times higher and 8 times lower than the rates estimated for the FA and AA assisted decompositions. Similarly, based on the MP2/aug-cc-pVTZ level

predicted results, it is seen that the rate for the H<sub>2</sub>O–assisted decomposition reaction is respectively 5 times higher and only 1.5 times lower with respect to the rates estimated for the FA and AA assisted decompositions. Furthermore, if the temperatures at 0 km altitude is 310 or 320K instead of 298.15K and the mixing ratio of the FA or AA is ~3.87 ppbv (which is the average mixing ratios of FA and AA and which is equivalent to  $6.1 \times 10^{10}$  molecules/cm<sup>3</sup>); it is seen that both the H<sub>2</sub>O and (H<sub>2</sub>O)<sub>2</sub> assisted H<sub>2</sub>CO<sub>3</sub> decompositions get relatively more and comparable impacts with both the FA and AA assisted decomposition reactions. Note that these are the predictions from the results obtained at the CCSD(T)/aug-cc-pVTZ level of theory. It is also worthwhile to note here that at the MP2/aug-cc-pVTZ level of theory and at 320K, the rate for the H<sub>2</sub>O–assisted H<sub>2</sub>CO<sub>3</sub> decomposition is respectively 13 and 2 times higher than the rates for the FA and AA assisted decomposition reactions, when we take the concentration of FA or AA  $\sim 6.1 \times 10^{10}$  molecules/cm<sup>3</sup> ( $\equiv 3.87$  ppbv). Therefore, and finally, the H<sub>2</sub>O–assisted H<sub>2</sub>CO<sub>3</sub>  $\rightarrow$  CO<sub>2</sub> + H<sub>2</sub>O decomposition reaction in comparison to the FA and AA assisted H<sub>2</sub>CO<sub>3</sub>  $\rightarrow$  CO<sub>2</sub> + H<sub>2</sub>O decomposition reactions is also expected to be important, especially, in the clean environment of Earth's atmosphere and/or at extremely hot and humid conditions. The calculated values of the relative rates for the H<sub>2</sub>O, (H<sub>2</sub>O)<sub>2</sub>, FA, AA, SA and HO<sub>2</sub> radical assisted H<sub>2</sub>CO<sub>3</sub> decompositions at the temperature 310 and 320 K have been given in the Supplementary Information. Similarly, in the higher altitude and up to 15 km, only the FA and/or AA assisted H<sub>2</sub>CO<sub>3</sub> decompositions are the dominant channels among the H<sub>2</sub>O, (H<sub>2</sub>O)<sub>2</sub>, FA, AA, SA and HO<sub>2</sub> radical assisted H<sub>2</sub>CO<sub>3</sub>  $\rightarrow$  CO<sub>2</sub> + H<sub>2</sub>O decomposition reactions. For example, with respect to the average concentrations of FA, (see Supplementary Information), it is seen from the CCSD(T)/aug-cc-pVTZ level predicted results that at the 5, 10 and 15 km altitudes of the Earth's atmosphere, the rates for the FA assisted H<sub>2</sub>CO<sub>3</sub> decompositions are respectively  $\sim 10^2$ ,  $10^4$  and  $10^6$  times higher than the rates associated with the H<sub>2</sub>O–assisted decomposition. It is also worth noting here that the OH radical initiated atmospheric

degradation of the gas-phase  $\text{H}_2\text{CO}_3$  molecule, which might be another important channel to look at the atmospheric loss of  $\text{H}_2\text{CO}_3$  molecule, has not been focused in this article.

Finally, as mentioned earlier that the  $\text{RCO}_2\text{H}$ -assisted  $\text{H}_2\text{CO}_3$  decomposition has been studied very recently by Kumar et al.<sup>42-43</sup> and the primary focus of this work was to explore the instability of the gaseous  $\text{H}_2\text{CO}_3$  molecule in presence of carboxylic acids, especially, at the 0 km altitude of the Earth's atmosphere. It has been pointed out from their M06-2X/aug-cc-pVTZ level predicted results including tunneling corrections that the formic acid (FA) assisted  $\text{H}_2\text{CO}_3$  decomposition is ~10 times faster than the  $\text{H}_2\text{O}$ -assisted  $\text{H}_2\text{CO}_3$  decomposition at 298.15 K. To reproduce this relative reaction rate, we also perform the M06-2X/aug-cc-pVTZ level of calculations for the water monomer, FA and AA assisted  $\text{H}_2\text{CO}_3$  decomposition reactions. It is seen from our calculations that although the M06-2X/aug-cc-pVTZ level optimized geometries of the pre-reactive complexes and transition states match well between their calculations and our calculations, nevertheless, there is somewhat inconsistency between their data and our data predicted at the same level of theory, especially, when we consider the comparison of calculated free energy values of the pre-reactive complexes and transition states with respect to the total free energies of isolated starting bimolecular reactants. It is worthwhile to note here that the dissimilarity in the optimized geometries of the exit channel complexes, which we have found when we have compared the optimized geometries of exist channel complexes, is not important here, as reaction rate calculation in forward direction does not depend upon the energetics of the exit channel complexes. Therefore, in Supplementary Information, we have provided a comparison between their data and our data associated with the pre-reactive complexes and transition states as well as the equations by which one can easily reproduce the values of reaction rates those we have given for the water monomer and FA assisted  $\text{H}_2\text{CO}_3$  decomposition reactions. From our calculations including tunneling corrections according to Gaussian-09 outputs, it is seen that at 298.15K the FA-assisted  $\text{H}_2\text{CO}_3$  decomposition is only ~2.7 times faster than the  $\text{H}_2\text{O}$ -assisted  $\text{H}_2\text{CO}_3$  decomposition. It is to be noted here that this

prediction is based on the concentrations of water and FA those have been reported by Kumar et al. and when the corrections with respect to the reaction degeneracy are not considered.

#### 4. Summary and Conclusion:

Carbonic acid ( $\text{H}_2\text{CO}_3$ ), a small molecule of six atoms involving three elements in the periodic table, is right at the interface between organic and inorganic chemistry. We note what has already been noted by other research groups that the detection of gas-phase interstellar  $\text{H}_2\text{CO}_3$  as well as in Earth's troposphere has become very challenging for a new generation of scientists and it is only hoped that one day, in near future, it will be detected as scientists get success in measuring the infrared spectra of the vapor phase  $\text{H}_2\text{CO}_3$  resulting from its polymorphs via the sublimations at cold temperatures.<sup>2,5-6,22</sup> Therefore, to understand the stability of the  $\text{H}_2\text{CO}_3$  molecule, especially, in the Earth's troposphere and lower stratosphere, we focus upon the energetics of the potential energy diagrams as well as the simple relative kinetics for the decomposition of  $\text{H}_2\text{CO}_3$  molecule into its constituents  $\text{CO}_2$  and  $\text{H}_2\text{O}$  molecules ( $\text{H}_2\text{CO}_3 \rightarrow \text{CO}_2 + \text{H}_2\text{O}$ ) via its shortest route in presence of various species those are present not only at significant trace levels in the Earth's atmosphere but also known as the effective catalysts in case of hydrogen atom transfer reactions in the doubly or multiply hydrogen-bonded interfaces via the O—H bond breaking and making process.<sup>46-48,77-83</sup> We have considered the  $\text{H}_2\text{CO}_3 \rightarrow \text{CO}_2 + \text{H}_2\text{O}$  decomposition reaction in presence of the one to three water ( $\text{H}_2\text{O}$ ) molecules as well as in presence of the formic acid (FA), acetic acid (AA), sulfuric acid (SA) and hydroperoxide ( $\text{HO}_2$ ) radical. Overall, fourteen different reaction pathways in terms of bimolecular encounters have been considered and the quantum chemistry calculations have been performed at the MP2/aug-cc-pVDZ, MP2/aug-cc-pVTZ, MP2/6-311++G(3df,3pd) and CCSD(T)/aug-cc-pVTZ levels of theories.

In conclusion, it is seen from our results that the most effective catalysts in the  $\text{H}_2\text{CO}_3 \rightarrow \text{CO}_2 + \text{H}_2\text{O}$  decomposition reaction are the FA, AA and SA, as the  $\text{H}_2\text{CO}_3 \rightarrow \text{CO}_2 + \text{H}_2\text{O}$  decomposition reaction in presence of these species are effectively the near-barrierless processes. However, by taking

the atmospheric concentrations of water monomer ( $\text{H}_2\text{O}$ ), dimer  $[(\text{H}_2\text{O})_2]$ , FA, AA, SA and  $\text{HO}_2$  radical, we find that the  $\text{H}_2\text{O}$  and  $(\text{H}_2\text{O})_2$  assisted  $\text{H}_2\text{CO}_3$  decomposition reactions are important channels to make the gas-phase  $\text{H}_2\text{CO}_3$  molecule unstable, especially, at 0 km altitude in clean environment of the Earth's atmosphere. This follows as the reaction rates for the  $\text{H}_2\text{O}$ ,  $(\text{H}_2\text{O})_2$ , FA and AA assisted  $\text{H}_2\text{CO}_3$  decompositions are comparable from each other within the factor 10. Similarly, at the 0 km altitude in polluted environment of the Earth's atmosphere and in the 5 to 15 km altitude range, only the FA and/or AA assisted decompositions are important. Therefore, up to 15 km altitude from the Earth's surface, both the SA and  $\text{HO}_2$  radical do not play any significant role in the  $\text{H}_2\text{CO}_3 \rightarrow \text{CO}_2 + \text{H}_2\text{O}$  decomposition reaction, even though the SA is also the effective catalyst like FA and AA. It is worth noting here that the OH radical initiated atmospheric degradation of the gas-phase  $\text{H}_2\text{CO}_3$  molecule, which might be another important channel to understand the atmospheric loss of  $\text{H}_2\text{CO}_3$  molecule, has not been focused in this article. Moreover, we have focused the  $\text{H}_2\text{CO}_3 \rightarrow \text{CO}_2 + \text{H}_2\text{O}$  decomposition mainly in the lower atmosphere of the Earth, and not in the outer space, where, especially, the  $\text{H}_2\text{SO}_4$  assisted  $\text{H}_2\text{CO}_3 \rightarrow \text{CO}_2 + \text{H}_2\text{O}$  decomposition reaction may have an important impact.

**Acknowledgement:** Financial support from the BARD project (PIC No: 12-R&D-SIN-5.04-0103), Department of Atomic Energy, Government of India, is gratefully acknowledged.

**Electronic Supplementary Information (ESI) Available:** The computed total electronic energies ( $E_{\text{total}}$ ), ZPE corrected electronic energies [ $E_{\text{total}}(\text{ZPE})$ ], imaginary frequencies of various Transition states (TS), rate constants as well as the other data as mentioned in the text. See DOI: 10.1039/b000000x/

**References:**

- 1 J. K. Terlouw, C. B. Lebrilla and H. Schwarz, *Angew. Chem. Int. Ed.*, 1987, **26**, 354-355.
- 2 S. E. Huber, S. Dalnodar, W. Kausch, S. Kimeswenger and M. Probst, *AIP Adv.*, 2012, **2**, 032180.
- 3 T. Mori, K. Suma, Y. Sumiyoshi and Y. Endo, *J. Chem. Phys.*, 2009, **130**, 204308.
- 4 T. Mori, K. Suma, Y. Sumiyoshi and Y. Endo, *J. Chem. Phys.*, 2011, **134**, 044319.
- 5 J. Bernard, M. Seidl, I. Kohl, K. R. Liedl, E. Mayer, O. Galvez, H. Grothe and T. Loerting, *Angew. Chem. Int. Ed.*, 2011, **50**, 1939-1943.
- 6 J. Bernard, R. G. Huber, K. R. Liedl, H. Grothe and T. Loerting, *J. Am. Chem. Soc.*, 2013, **135**, 7732-7737.
- 7 N. DelloRusso, R. K. Khanna and M. H. Moore, *J. Geophys. Res., [Planets]* 1993, **98**, 5505-5510.
- 8 M. H. Moore, R. Khanna and B. Donn, *J. Geophys. Res., [Planets]* 1991, **96**, 17541-17545.
- 9 M. H. Moore and R. K. Khanna, *Spectrochim. Acta, Part A*, 1991, **47A**, 255-262.
- 10 J. R. Brucato, M. E. Palumbo and G. Strazzulla, *Icarus*, 1997, **125**, 135-144.
- 11 G. Strazzulla, G. Leto, F. Spinella and O. Gomis, *Astrobiology*, 2005, **5**, 612-621.
- 12 P. A. Gerakines, M. H. Moore and R. L. Hudson, *Astron. Astrophys.*, 2000, **357**, 793-800.
- 13 C. Y. R. Wu, D. L. Judge, B.-M. Cheng, T.-S. Yih, C. S. Lee and W. H. Ip, *J. Geophys. Res., [Planets]* 2003, **108**, 5032.
- 14 M. Garozzo, D. Fulvio, O. Gomis, M. E. Palumbo and G. Strazzulla, *Planet. Space Sci.*, 2008, **56**, 1300-1308.
- 15 Y. Oba, N. Watanabe, A. Kouchi, T. Hama and V. Pirronello, *Astrophys. J.*, 2010, **722**, 1598-1606.
- 16 J. S. Lewis and D. H. Grinspoon, *Science*, 1990, **249**, 1273-1275.

- 17 N. DelloRusso, R. K. Khanna and M. H. Moore, *J. Geophys. Res., [Planets]* 1993, **98**, 5505-5510.
- 18 R. K. Khanna, J. A. Tossell and K. Fox, *Icarus*, 1994, **112**, 541-544.
- 19 W. Hage, A. Hallbrucker and E. Mayer, *J. Chem. Soc. Faraday Trans.*, 1995, **91**, 2823-2826.
- 20 G. Strazzulla, J. R. Brucato, G. Cimino and M. E. Palumbo, *Planet. Space Sci.*, 1996, **44**, 1447-1450.
- 21 W. Hage, K. R. Liedl, A. Hallbrucker and E. Mayer, *Science*, 1998, **279**, 1332-1335.
- 22 R. L. Hudson, *J. Chem. Educ.*, 2006, **83**, 1611-1616.
- 23 Z. Peeters, R. L. Hudson, M. H. Moore and A. Lewis, *Icarus*, 2010, **210**, 480-487.
- 24 H. Falcke and S. H. Eberle, *Water Res.*, 1990, **24**, 685-688.
- 25 K. Adamczyk, M. Premont-Schwarz, D. Pines, E. Pines and E. T. J. Nibbering, *Science*, 2009, **326**, 1690-1694.
- 26 W. Hage, A. Hallbrucker and E. Mayer, *J. Am. Chem. Soc.*, 1993, **115**, 8427-8431.
- 27 K. Winkel, W. Hage, T. Loerting, S. L. Price and E. Mayer, *J. Am. Chem. Soc.*, 2007, **129**, 13863-13871.
- 28 I. Kohl, K. Winkel, M. Bauer, K. R. Liedl, T. Loerting and E. Mayer, *Angew. Chem. Int. Ed.*, 2009, **48**, 2690-2694.
- 29 C. Mitterdorfer, J. Bernard, F. Klauser, K. Winkel, I. Kohl, K. R. Liedl, H. Grothe, E. Mayer and T. Loerting, *J. Raman Spectrosc.*, 2012, **43**, 108-115.
- 30 S. K. Reddy, C. H. Kulkarni and S. Balasubramanian, *J. Phys. Chem. A*, 2012, **116**, 1638-1647.
- 31 J. Murillo, J. David and A. Restrepo, *Phys. Chem. Chem. Phys.*, 2010, **2**, 10963-10970.
- 32 T. Loerting and J. Bernard, *ChemPhysChem*, 2010, **11**, 2305-2309.
- 33 J. Bernard, M. Seidl, E. Mayer and T. Loerting, *ChemPhysChem*, 2012, **13**, 3087-3091.
- 34 A. G. Galinos and A. A. Carotti, *J. Am. Chem. Soc.*, 1961, **63**, 752-752.
- 35 G. Gattow and U. Gerwarth, *Angew. Chem. Int. Ed.*, 1965, **4**, 149-149.

- 36 H. P. Reisenauer, J. P. Wagner, and P. R. Schreiner, *Angew. Chem. Int. Ed.*, 2014, **53**, 11766-11771.
- 37 Y. Oba, N. Watanabe, A. Kouchi, T. Hama and V. Pirronello, *Phys. Chem. Chem. Phys.*, 2011, **13**, 15792-15797.
- 38 S. Ghoshal and M. K. Hazra, *J. Phys. Chem. A*, 2014, **118**, 2385-2392.
- 39 Loerting, T.; Tautermann, C.; Kroemer, R. T.; Kohl, I.; Hallbrucker, A.; Mayer, E.; Liedl, K. R., *Angew. Chem. Int. Ed.*, 2000, **39**, 891-894.
- 40 C. S. Tautermann, A. F. Voegele, T. Loerting, I. Kohl, A. Hallbrucker, E. Mayer and K. R. Liedl, *Chem. Eur. J.*, 2002, **8**, 66-73.
- 41 S. A. de Marothy, *Int. J. Quant. Chem.*, 2013, **113**, 2306-2311.
- 42 M. Kumar, D. H. Busch, B. Subramaniam and W. H. Thompson, *J. Phys. Chem. A*, 2014, **118**, 5020-5028.
- 43 M. Kumar, D. H. Busch, B. Subramaniam and W. H. Thompson, *J. Phys. Chem. A*, 2014, **118**, 10155-10156.
- 44 S. G. Lakkis, M. Lavorato and P. O. Canziani, *Atmospheric Research*, 2009, **92**, 18-26.
- 45 R. Spang, G. Günther, M. Riese, L. Hoffmann, R. Müller, and S. Griessbach, *Atmos. Chem. Phys. Discuss.*, 2014, **14**, 12323-12375.
- 46 R. J. Buszek, A. Sinha and J. S. Francisco, *J. Am. Chem. Soc.*, 2011, **133**, 2013-2015.
- 47 J. S. Francisco, M. Torrent-Sucarrat and J. M. Anglada, *J. Am. Chem. Soc.*, 2012, **134**, 20632-20644.
- 48 J. Gonzalez, M. Torrent-Sucarrat and J. M. Anglada, *Phys. Chem. Chem. Phys.*, 2010, **12**, 2116-2125.
- 49 M. J. Frisch, G. W. Trucks, H. B. Schlegel, G. E. Scuseria, M. A. Robb, J. R. Cheeseman, G. Scalmani, V. Barone, B. Mennucci and G. A. Petersson. H. Nakatsuji, M. Caricato, X. Li, H. P. Hratchian, A. F. Izmaylov, J. Bloino, G. Zheng, J. L. Sonnenberg, M. Hada, M. Ehara, K.

- Toyota, R. Fukuda, J. Hasegawa, M. Ishida, T. Nakajima, Y. Honda, O. Kitao, H. Nakai, T. Vreven, J. A. Montgomery Jr, J. E. Peralta, F. Ogliaro, M. Bearpark, J. J. Heyd, E. Brothers, K. N. Kudin, V. N. Staroverov, R. Kobayashi, J. Normand, K. Raghavachari, A. Rendell, J. C. Burant, S. S. Iyengar, J. Tomasi, M. Cossi, N. Rega, J. M. Millam, M. Klene, J. E. Knox, J. B. Cross, V. Bakken, C. Adamo, J. Jaramillo, R. Gomperts, R. E. Stratmann, O. Yazyev, A. J. Austin, R. Cammi, C. Pomelli, J. W. Ochterski, R. L. Martin, K. Morokuma, V. G. Zakrzewski, G. A. Voth, P. Salvador, J. J. Dannenberg, S. Dapprich, A. D. Daniels, Farkas, J. B. Foresman, J. V. Ortiz, J. Cioslowski and D. J. Fox, *Gaussian 09*, Revision B.01, Gaussian, Inc., Wallingford, CT, 2010.
- 50 J. R. Alvarez-Idaboy and A. Galano, *Theor. Chem. Acc.*, 2010, **126**, 75-85.
- 51 K. R. Liedl, S. Sekusak and E. Mayer, *J. Am. Chem. Soc.*, 1997, **119**, 3782-3784.
- 52 B. Reimann, K. Buchhold, H.-D. Barth, H.-D. Brutschy, P. Tarakeshwar and K. S. Kim, *J. Chem. Phys.*, 2002, **117**, 8805-8822.
- 53 P. P. Kumar, A. G. Kalinichev and R. J. Kirkpatrick, *J. Chem. Phys.*, 2007, **126**, 204315.
- 54 P. Ballone, B. Montanari and R. O. Jones, *J. Chem. Phys.*, 2000, **112**, 6571-6575.
- 55 S. Ghoshal and M. K. Hazra, *J. Phys. Chem. A*, 2014, **118**, 4620-4630.
- 56 A. Razavi, F. Karagulian, L. Clarisse, D. Hurtmans, P. F. Coheur, C. Clerbaux, J. F. Müller and T. Stavrou, *Atmos. Chem. Phys.*, 2011, **11**, 857-872.
- 57 M. W. Shephard, A. Goldman, S. A. Clough and E. J. Mlawer, *J. Quant. Spectrosc. Radiat. Transfer.*, 2003, **82**, 383-390.
- 58 J. E. Lawrence and P. Koutrakls, *Environ. Sci. Technol.*, 1994, **28**, 957-964.
- 59 S. R. Souza and L. R. F. Carvalho, *J. Braz. Chem. Soc.*, 2001, **12**, 755-762.
- 60 M. Grutter, N. Glatthor, G. P. Stiller, H. Fischer, U. Grabowski, M. Höpfner, S. Kellmann, A. Linden and T. von Clarmann, *J. Geophys. Res., [Atmospheres]* 2010, **115**, D1030.

- 61 G. González Abad, P. F. Bernath, C. D. Boone, S. D. McLeod, G. L. Manney and G. C. Toon, *Atmos. Chem. Phys.*, 2009, **9**, 8039-8047.
- 62 S. R. Souza, P. C. Vasconcellos and L. R. F. Carvalho, *Atmos. Environ.*, 1999, **33**, 2563-2574.
- 63 R. W. Talbot, J. E. Dibb, B. L. Lefer, E. M. Scheuer, J. D. Bradshaw, S. T. Sandholm, S. Smyth, D. R. Blake, N. J. Blake, G. W. Sachse, J. E. Collins and G. L. Gregory, *J. Geophys. Res.*, 1997, **102**, 28303-28313.
- 64 E. Sanhueja, L. Figuera and M. Santana, *Atmos. Environ.*, 1996, **30**, 1861-1873.
- 65 A. Chebbi and P. Carlier, *Atmos. Environ.*, 1996, **30**, 4233-4249.
- 66 P. Khare, G. S. Satsangi, N. Kumar, K. M. Kumari and S. S. Srivastav, *Atmos. Environ.*, 1997, **31**, 3867-3875.
- 67 K. Granby and C. S. Christensen, *Atmos. Environ.*, 1997, **31**, 1403-1415.
- 68 T. Reiner, O. Möhler and F. Arnold, *J. Geophys. Res.*, 1999, **104**, 13943-13952.
- 69 M. O. Andreae, R. W. Talbot, T. W. Andreae and R. C. Harris, *J. Geophys. Res.*, 1988, **93**, 1616-1624.
- 70 R. P. Turco, P. Hamill, O. B. Toon, R. C. Whitten and C. S. King, *J. Atmos. Sci.*, 1979, **36**, 699-717.
- 71 M. J. Mills, O. B. Toon, V. Vaida, P. E. Hintze, H. G. Kjaergaard, D. P. Schofield and T. W. Robinson, *J. Geophys. Res.*, 2005, **110**, D08201.
- 72 J. Mao, D. J. Jacob, M. J. Evans, J. R. Olson, X. Ren, W. H. Brune, J. M. S. Clair, J. D. Crouse and K. M. Spencer, M. R. Beaver, P. O. Wennberg, M. J. Cubison, J. L. Jimenez, A. Fried, P. Weibring, J. G. Walega, S. R. Hall, A. J. Weinheimer, R. C. Cohen, G. Chen, J. H. Crawford, C. McNaughton, A. D. Clarke, L. Jaegle, J. A. Fisher, R. M. Yantosca, P. Le Sager and C. Carouge, *Atmos. Chem. Phys.*, 2010, **10**, 5823-5838.

- 73 D. Kubistin, H. Harder, M. Martinez, M. Rudolf, R. Sander, H. Bozem, G. Eerdeken, H. Fischer, C. Gurk and T. Klüpfel. R. K. onigstedt, U. Parchatka, C. L. Schiller, A. Stickler, D. Taraborrelli, J. Williams and J. Lelieveld, *Atmos. Chem. Phys.*, 2010, **10**, 9705-9728.
- 74 G. P. Brasseur and S. Solomon, *Aeronomy of the Middle Atmosphere*, Springer, Netherlands, 2005.
- 75 W. B. DeMore, S. P. Sander, D. M. Golden, R. F. Hampson, M. J. Kurylo, C. J. Howard, A. R. Ravishankara, C. E. Kolb and M. J. Molina, JPL Publication 97-4, Jet Propulsion Laboratory, California Institute of Technology, Pasadena, CA, 1997.
- 76 J. M. Anglada, G. J. Hoffman, L. V. Slipchenko, M. M. Costa, M. F. Ruiz-López and J. S. Francisco, *J. Phys. Chem. A*, 2013, **117**, 10381-10396.
- 77 M. K. Hazra and A. Sinha, *J. Am. Chem. Soc.*, 2011, **133**, 17444-17453.
- 78 B. Long, Z-w. Long, Y-b. Wang, X-f. Tan, Y-h. Han, C-y. Long, S-j. Qin and W-j. Zhang, *Chem. Phys. Chem.*, 2012, **13**, 323-329.
- 79 M. K. Hazra, J. S. Francisco and A. Sinha, *J. Phys. Chem. A*, 2013, **117**, 11704-11710.
- 80 M. K. Hazra, J. S. Francisco and A. Sinha, *J. Phys. Chem. A*, 2014, **118**, 4095-4105.
- 81 G. da Silva, *Angew. Chem. Int. Ed.*, 2010, **49**, 7523-7525.
- 82 M. K. Hazra and T. Chakraborty, *J. Phys. Chem. A*, 2005, **109**, 7621-7625.
- 83 M. K. Hazra and T. Chakraborty, *J. Phys. Chem. A*, 2006, **110**, 9130-9136.
- 84 H. Eyring, *J. Chem. Phys.*, 1935, **3**, 107-115.
- 85 M. G. Evans and M. Polanyi, *Trans. Faraday Soc.*, 1935, **31**, 875-894.
- 86 D. G. Truhlar, W. L. Hase and J. T. Hynes, *J. Phys. Chem.*, 1983, **87**, 2664-2682.
- 87 C. Eckart, *Phys. Rev.*, 1930, **35**, 1303-1309.
- 88 R. L. Brown, *J. Res. Natl. Bur. Stand., (U.S.)* 1981, **86**, 357-359.
- 89 H. S. Johnston and J. Heicklen, *J. Phys. Chem.*, 1962, **66**, 532-533.

- 90 L. Arnaut, S. Formosinho and H. Burrows, *Chemical Kinetics from Molecular Structure to Chemical Reactivity*, Elsevier, Netherlands, 2007.
- 91 D. A. McQuarrie, *Statistical Thermodynamics*, Harper and Row, New York, 1973.
- 92 G. J. Frost and V. Vaida, *J. Geophys. Res.*, 1995, **100**, 18803-18809.

**Table 1:** Zero point vibrational energy (ZPE) corrected binding energies (kcal/mol) of all the complexes at the MP2 level of theory in conjunction with aug-cc-pVDZ, aug-cc-pVTZ and 6-311++G(3df,3pd) basis sets as well as at the CCSD(T)/aug-cc-pVTZ level of calculations. The binding energies of all the pre-reactive complexes (**RC-I to RC-XIII**) have been calculated in terms of bimolecular encounters between two reactants (monomers/complexes) as given in the 1<sup>st</sup> column of the table. For an example, in the case of **RC-III**, the binding energy has been calculated by subtracting the total electronic energies of the **RC-I** + H<sub>2</sub>O reactants from the calculated energy of the **RC-III**. In case of exit channel product complexes (**PC-I to PC-XIII**), except other than those labeled below, the binding energies have been calculated by subtracting the total electronic energies of all the monomers forming the complex from the calculated energy of that complex. Normal mode vibrational frequency calculations at the MP2/aug-cc-pVDZ, MP2/aug-cc-pVTZ and MP2/6-311++G(3df,3pd) level have been performed to estimate the respective zero point energy (ZPE) corrections. The ZPE correction in case of CCSD(T)/aug-cc-pVTZ level of calculations have been done from the MP2/aug-cc-pVTZ level predicted ZPE correction.

Complexes	MP2/ aug-cc-pVDZ	MP2/ aug-cc-pVTZ	MP2/ 6-311++G(3df,3pd)	CCSD(T)/ aug-cc-pVTZ
RC-I (H <sub>2</sub> CO <sub>3</sub> + H <sub>2</sub> O)	7.33	7.25	7.23	7.22
RC-II [(H <sub>2</sub> CO <sub>3</sub> + (H <sub>2</sub> O) <sub>2</sub> ]	11.36	11.33	11.26	11.16
RC-II (RC-I + H <sub>2</sub> O)	7.18	7.16	7.12	7.06
RC-III (RC-I + H <sub>2</sub> O)	9.64	9.68	9.64	---
RC-IV (RC-I + H <sub>2</sub> O)	6.56	6.42	6.40	---
RC-V (RC-II + H <sub>2</sub> O)	10.12	10.13	10.11	---
RC-VI [(RC-I + (H <sub>2</sub> O) <sub>2</sub> ]	16.25	16.32	16.36	---
RC-VII [(RC-I + (H <sub>2</sub> O) <sub>2</sub> ]	13.36	13.13	13.16	---
RC-VIII [(RC-I + (H <sub>2</sub> O) <sub>2</sub> ]	13.35	13.20	13.27	---
RC-IX [(H <sub>2</sub> CO <sub>3</sub> + (H <sub>2</sub> O) <sub>3</sub> ]	8.74	8.58	8.55	---
RC-X (H <sub>2</sub> CO <sub>3</sub> + FA)	10.86	11.01	10.87	11.01
RC-XI (H <sub>2</sub> CO <sub>3</sub> + AA)	11.90	12.04	11.87	12.08
RC-XII (H <sub>2</sub> CO <sub>3</sub> + SA)	11.09	11.50	11.69	11.54
RC-XIII (H <sub>2</sub> CO <sub>3</sub> + HO <sub>2</sub> )	8.93	8.91	9.01	8.66
PC-I	7.38	7.15	7.11	7.44
PC-II	14.31 (3.29) <sup>a</sup>	13.97 (3.11) <sup>a</sup>	14.00 (3.11) <sup>a</sup>	14.23
PC-III	11.23	10.84	10.78	---
PC-IV	14.18 (3.16) <sup>a</sup>	13.86 (3.00) <sup>a</sup>	13.87 (2.99) <sup>a</sup>	---
PC-V	19.44 (8.42) <sup>c</sup>	18.96 (8.10) <sup>c</sup>	18.97 (8.08) <sup>c</sup>	---
PC-VI	19.44	18.96	18.97	---
PC-VII	24.28 (3.79) <sup>b</sup>	23.74 (3.44) <sup>b</sup>	23.89 (3.43) <sup>b</sup>	---
PC-VIII	23.78 (3.28) <sup>b</sup>	23.37 (3.07) <sup>b</sup>	23.50 (3.04) <sup>b</sup>	---
PC-IX	19.15 (8.13) <sup>c</sup>	18.69 (7.84) <sup>c</sup>	18.68 (7.79) <sup>c</sup>	---
PC-X	9.92	9.80	9.71	10.21
PC-XI	10.37	10.21	10.08	10.66
PC-XII	13.84	11.01	11.18	11.48
PC-XIII	9.29	8.98	9.09	9.03

<sup>a</sup> Binding energy of the CO<sub>2</sub>···(H<sub>2</sub>O)<sub>3</sub> complex, when it is formed from the bimolecular encounters between the CO<sub>2</sub> + (H<sub>2</sub>O)<sub>3</sub> reactants. <sup>b</sup> Binding energy of the CO<sub>2</sub>···(H<sub>2</sub>O)<sub>4</sub> complex, when it is formed from the bimolecular encounters between the CO<sub>2</sub> + (H<sub>2</sub>O)<sub>4</sub> reactants. <sup>c</sup> Binding energy of CO<sub>2</sub>···(H<sub>2</sub>O)<sub>4</sub> complex, when it is formed, from the ternary encounters between the CO<sub>2</sub> + (H<sub>2</sub>O)<sub>3</sub> + H<sub>2</sub>O reactants.

**Table 2:** Zero point vibrational energy (ZPE) corrected barrier heights (kcal/mol) for various unimolecular decomposition steps associated with the reaction pathways from **R-I** to **R-XIII**, as labeled in the 1<sup>st</sup> column of table, at the MP2/aug-cc-pVDZ, MP2/aug-cc-pVTZ and MP2/6-311++G(3df,3pd) level of calculations as well as at the CCSD(T)/aug-cc-pVTZ level of calculations. The values in parenthesis are the relative energies of the transition states (**TS-I** to **TS-XIII**) with respect to reactants those are involved in bimolecular encounters as discussed in the text. For an example, in the case of reaction pathway: **R-I**, the MP2/aug-cc-pVTZ level of calculation incorporating ZPE correction predict that the **TS-I** is being 13.50 kcal/mol higher in energy (indicated by positive sign) than the total energy of the H<sub>2</sub>CO<sub>3</sub> + H<sub>2</sub>O reactants. Normal mode vibrational frequency calculations at the MP2/aug-cc-pVDZ, MP2/aug-cc-pVTZ and MP2/6-311++G(3df,3pd) levels have been performed to estimate the respective zero point energy (ZPE) corrections. The ZPE corrections in case of the CCSD(T)/aug-cc-pVTZ level of calculations have been done from the MP2/aug-cc-pVTZ level predicted ZPE corrections.

Transition States	MP2/ aug-cc-pVDZ	MP2/ aug-cc-pVTZ	MP2/6- 311++G(3df,3pd)	CCSD(T)/ aug-cc-pVTZ
TS-I [R-I $\equiv$ H <sub>2</sub> CO <sub>3</sub> + H <sub>2</sub> O]	20.93 (+13.60)	20.69 (+13.50)	21.25 (+14.02)	23.36 (+16.14)
TS-II [R-II $\equiv$ H <sub>2</sub> CO <sub>3</sub> + (H <sub>2</sub> O) <sub>2</sub> ]	17.52 (+6.16)	16.97 (+5.64)	17.25 (+5.99)	19.55 (+8.39)
TS-II [R-IIa $\equiv$ RC-I + H <sub>2</sub> O]	17.52 (+10.34)	16.97 (+9.82)	17.25 (+10.13)	---
TS-III [R-III $\equiv$ RC-I + H <sub>2</sub> O]	20.38 (+10.74)	19.98 (+10.30)	20.48 (+10.83)	---
TS-IV [R-IV $\equiv$ RC-I + H <sub>2</sub> O]	19.53 (+12.97)	19.61 (+13.19)	20.14 (+13.74)	---
TS-V [R-V $\equiv$ RC-II + H <sub>2</sub> O]	17.13 (+7.02)	16.39 (+6.26)	16.64 (+6.53)	---
TS-VI [R-VI $\equiv$ RC-I + (H <sub>2</sub> O) <sub>2</sub> ]	19.89 (+3.64)	19.34 (+3.02)	19.77 (+3.41)	---
TS-VII [R-VII $\equiv$ RC-I + (H <sub>2</sub> O) <sub>2</sub> ]	16.52 (+3.17)	16.53 (+3.40)	17.09 (+3.93)	---
TS-VIII [R-VIII $\equiv$ RC-I + (H <sub>2</sub> O) <sub>2</sub> ]	16.83 (+3.48)	16.84 (+3.64)	17.37 (+4.10)	---
TS-IX [R-IX $\equiv$ H <sub>2</sub> CO <sub>3</sub> + (H <sub>2</sub> O) <sub>3</sub> ]	19.24 (+10.49)	19.23 (+10.65)	19.71 (+11.16)	---
TS-X [R-X $\equiv$ H <sub>2</sub> CO <sub>3</sub> + FA]	12.46 (+1.60)	12.24 (+1.23)	12.47 (+1.60)	14.37 (+3.36)
TS-XI [R-XI $\equiv$ H <sub>2</sub> CO <sub>3</sub> + AA]	11.98 (+0.08)	11.89 (-0.15)	12.05 (+0.18)	13.92 (+1.84)
TS-XII [R-XII $\equiv$ H <sub>2</sub> CO <sub>3</sub> + SA]	12.05 (+0.96)	11.56 (+0.06)	11.75 (+0.06)	13.85 (+2.31)
TS-XIII [R-XIII $\equiv$ H <sub>2</sub> CO <sub>3</sub> + HO <sub>2</sub> ]	9.36 (+0.43)	9.58 (+0.67)	9.78 (+0.77)	15.56 (+6.9)

**Table 3:** The MP2/aug-cc-pVTZ level predicted reaction rates for the various reaction pathways in presence of one to three water molecules with respect to the rate estimated for the H<sub>2</sub>O–assisted H<sub>2</sub>CO<sub>3</sub> decomposition reaction ( $v_I$ ). The reaction rates ( $v_I$  to  $v_{VIII}$ ) for the various reaction pathways have been labeled according to the various pre-reactive complexes (**RC-I to RC-VIII**), as mentioned in the text. The values given in the parenthesis correspond to the results predicted at the CCSD(T)/aug-cc-pVTZ level of calculations. Temperatures and pressures at different altitudes of the Earth’s atmosphere have been taken from Ref-92.

Altitude (km)	T (K)	( $v_I/v_I$ )	( $v_{II}/v_I$ ) <sup>a</sup>	( $v_{IIa}/v_I$ ) <sup>a</sup>	( $v_{III}/v_I$ )	( $v_{IV}/v_I$ )	( $v_V/v_I$ )	( $v_{VI}/v_I$ )	( $v_{VII}/v_I$ )	( $v_{VIII}/v_I$ )
0	298.15	1.0 (1.0)	$5.0 \times 10^{-1}$ ( $4.4 \times 10^{-1}$ )	$3.9 \times 10^{-1}$	$2.5 \times 10^{-1}$	$3.2 \times 10^{-3}$	$3.7 \times 10^{-1}$	$1.7 \times 10^{-1}$	$4.4 \times 10^{-2}$	$3.8 \times 10^{-2}$
5	259.3	1.0 (1.0)	$2.3 \times 10^{-1}$ ( $1.9 \times 10^{-1}$ )	$1.8 \times 10^{-1}$	$1.5 \times 10^{-1}$	$5.9 \times 10^{-4}$	$1.2 \times 10^{-1}$	$0.5 \times 10^{-1}$	$0.9 \times 10^{-2}$	$0.7 \times 10^{-2}$
10	229.7	1.0 (1.0)	$3.5 \times 10^{-2}$ ( $2.7 \times 10^{-2}$ )	$2.8 \times 10^{-2}$	$3.4 \times 10^{-2}$	$3.8 \times 10^{-5}$	$5.5 \times 10^{-3}$	$2.6 \times 10^{-3}$	$2.9 \times 10^{-4}$	$2.2 \times 10^{-4}$
15	212.6	1.0 (1.0)	$5.0 \times 10^{-3}$ ( $0.3 \times 10^{-2}$ )	$4.1 \times 10^{-3}$	$7.2 \times 10^{-3}$	$3.1 \times 10^{-6}$	$2.2 \times 10^{-4}$	$1.0 \times 10^{-4}$	$8.5 \times 10^{-6}$	$0.6 \times 10^{-5}$

<sup>a</sup>  $v_{II}$  and  $v_{IIa}$  are corresponding to the rates of the reaction pathways where the water dimer and two water molecules actively assist the H<sub>2</sub>CO<sub>3</sub> decomposition by a common pre-reactive complex (**RC-II**).

**Table 4:** The MP2/aug-cc-pVTZ level predicted reaction rates for the various reaction pathways in presence of H<sub>2</sub>O, formic acid (FA), acetic acid (AA), sulfuric acid (SA) and hydroperoxide (HO<sub>2</sub>) radical with respect to the rate estimated for the H<sub>2</sub>O–assisted H<sub>2</sub>CO<sub>3</sub> decomposition reaction ( $v_I$ ). The reaction rates ( $v_X$  to  $v_{XIII}$ ) for the various reaction pathways have been labeled according to the various pre-reactive complexes (**RC-X** to **RC-XIII**) and  $v_X$ ,  $v_{XI}$ ,  $v_{XII}$  and  $v_{XIII}$  are respectively the rates for the FA, AA, SA and HO<sub>2</sub> radical assisted H<sub>2</sub>CO<sub>3</sub> decomposition reactions. The values given in the parenthesis correspond to the results predicted at the CCSD(T)/aug-cc-pVTZ level of calculations. Temperatures and pressures at different altitudes of the Earth’s atmosphere have been taken from Ref-92.

Altitude (km)	T (K)	( $v_I/v_I$ )	( $v_X/v_I$ )	( $v_{XI}/v_I$ )	( $v_{XII}/v_I$ )	( $v_{XIII}/v_I$ )
0	298.15	1.0 (1.0)	0.9 (3.2)	7.7 (40.7)	0.003 (0.02)	0.015 ( $8.6 \times 10^{-5}$ )
5	259.3	1.0 (1.0)	55 ( $2.2 \times 10^2$ )	$4.8 \times 10^2$ ( $3.5 \times 10^3$ )	0.41 (2.82)	1.6 ( $4.9 \times 10^{-3}$ )
10	229.7	1.0 (1.0)	$0.9 \times 10^4$ ( $4.5 \times 10^4$ )	$8.8 \times 10^4$ ( $8.0 \times 10^5$ )	$2.3 \times 10^1$ ( $2.2 \times 10^2$ )	$0.9 \times 10^3$ (1.7)
15	212.6	1.0 (1.0)	$3.1 \times 10^5$ ( $1.7 \times 10^6$ )	$3.3 \times 10^6$ ( $3.5 \times 10^7$ )	$6.3 \times 10^1$ ( $7.0 \times 10^2$ )	$1.4 \times 10^4$ ( $1.8 \times 10^1$ )

## Figure Captions:

**Figure 1:** Visualization of the shortest routes for the decomposition of isolated carbonic acid (A) and decomposition of carbonic acid in presence of water, formic acid and carbonic acid (B to D) via either intramolecular or intermolecular hydrogen transfer processes.

**Figure 2:** The MP2/aug-cc-pVTZ level optimized geometries of the two most stable conformers of carbonic acid ( $\text{H}_2\text{CO}_3$ ).

**Figure 3:** Potential energy profiles for the decomposition of the isolated  $\text{H}_2\text{CO}_3$  molecule (red color) and for water monomer assisted  $\text{H}_2\text{CO}_3$  decomposition (blue color). The energy profiles have been calculated at the MP2/aug-cc-pVTZ level of theory including zero point vibration energy (ZPE) corrections.

**Figure 4:** The MP2/aug-cc-pVTZ level optimized geometries of the three different entrance channel pre-reactive  $\text{H}_2\text{CO}_3 \cdots \text{H}_2\text{O} \cdots \text{H}_2\text{O}$  complexes (**RC-II, III and IV**) and their corresponding three exit channel  $\text{CO}_2 \cdots \text{H}_2\text{O} \cdots \text{H}_2\text{O} \cdots \text{H}_2\text{O}$  product complexes (**PC-II, III and IV**) and transition states (**TS-II, III and IV**) associated with the two water molecules assisted  $\text{H}_2\text{CO}_3 \rightarrow \text{CO}_2 + \text{H}_2\text{O}$  decomposition reaction.

**Figure 5:** The MP2/aug-cc-pVTZ level predicted and ZPE corrected four different potential energy profiles for the  $\text{H}_2\text{CO}_3 \rightarrow \text{CO}_2 + \text{H}_2\text{O}$  decomposition reaction in presence of two water molecules those are associated with the **RC-II, III and IV**. The potential energy profile associated with the  $\text{H}_2\text{CO}_3 + \text{H}_2\text{O} \cdots \text{H}_2\text{O}$  reactant channel has been shown in the section (A) and the three different potential energy profiles for the  $\text{H}_2\text{CO}_3 \cdots \text{H}_2\text{O} + \text{H}_2\text{O}$  reactants have been shown in the section (B).

**Figure 6:** The MP2/aug-cc-pVTZ level optimized geometries of the five different entrance channel pre-reactive  $\text{H}_2\text{CO}_3 \cdots \text{H}_2\text{O} \cdots \text{H}_2\text{O} \cdots \text{H}_2\text{O}$  complexes (**RC-V, VI, VII, VIII and IX**) and their corresponding five exit channel  $\text{CO}_2 \cdots \text{H}_2\text{O} \cdots \text{H}_2\text{O} \cdots \text{H}_2\text{O} \cdots \text{H}_2\text{O}$  product complexes (**PC-V, VI, VII, VIII and IX**) and transition states (**TS-V, VI, VII, VIII and IX**) associated with the three water molecules assisted  $\text{H}_2\text{CO}_3 \rightarrow \text{CO}_2 + \text{H}_2\text{O}$  decomposition reaction.

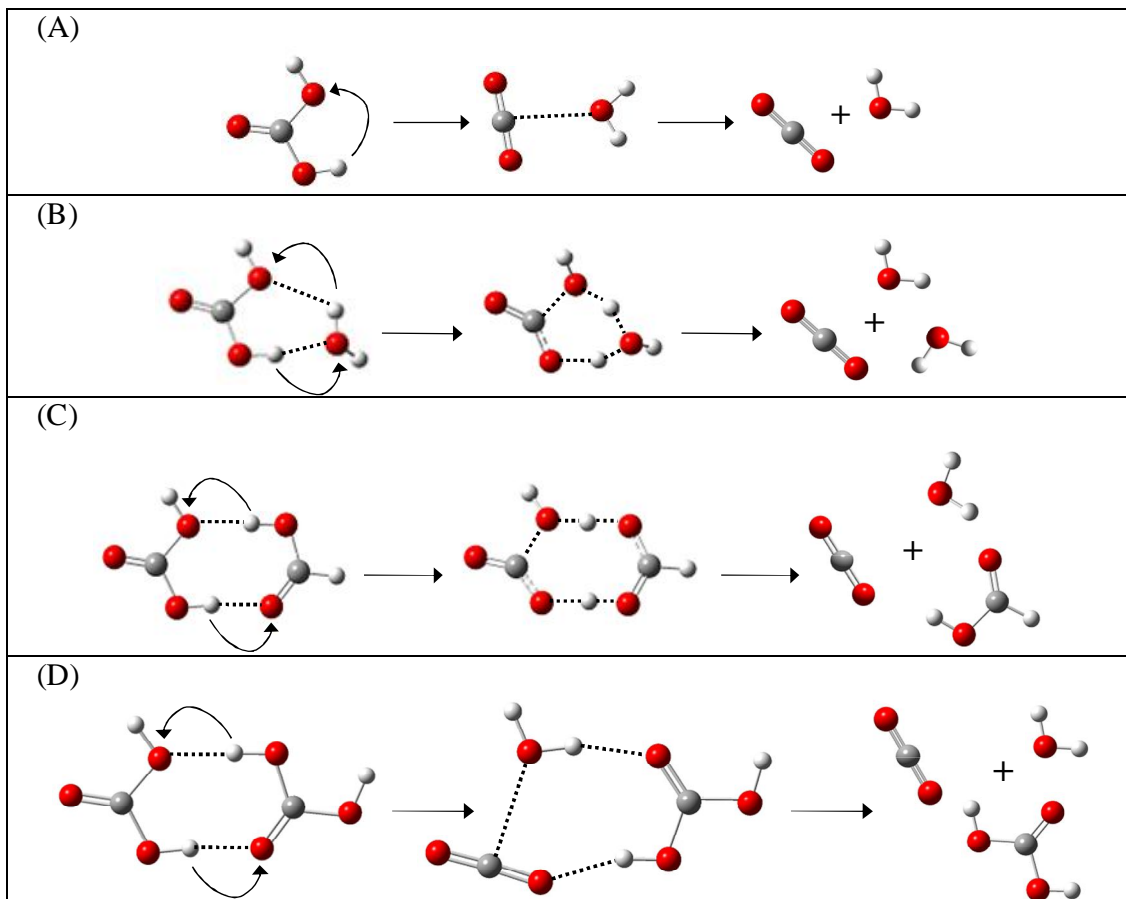
**Figure 7:** The MP2/aug-cc-pVTZ level predicted and ZPE corrected five different potential energy profiles for the  $\text{H}_2\text{CO}_3 \rightarrow \text{CO}_2 + \text{H}_2\text{O}$  decomposition reaction in presence of three water molecules those are associated with the **RC-V, VI, VII, VIII and IX**. (A) The potential energy profile for the  $\text{H}_2\text{CO}_3 \cdots \text{H}_2\text{O} \cdots \text{H}_2\text{O} + \text{H}_2\text{O}$  reactants that results in the **RC-V**. (B) The three different potential energy profiles for the  $\text{H}_2\text{CO}_3 \cdots \text{H}_2\text{O} + \text{H}_2\text{O} \cdots \text{H}_2\text{O}$  reactants those result in **RC-VI, VII, VIII**. (C) The potential energy profile for the  $\text{H}_2\text{CO}_3 + (\text{H}_2\text{O})_3$  reactants that results in the **RC-IX**.

**Figure 8:** The MP2/aug-cc-pVTZ level optimized geometries of the entrance channel pre-reactive complexes (**RC-X, XI, XII and XIII**), exit channel product complexes (**PC-X, XI, XII and XIII**) and transition states (**TS-X, XI, XII and XIII**) associated with the formic acid (FA), acetic acid (AA), sulfuric acid (SA) and hydroperoxide ( $\text{HO}_2$ ) radical assisted  $\text{H}_2\text{CO}_3 \rightarrow \text{CO}_2 + \text{H}_2\text{O}$  decomposition reactions.

**Figure 9:** (A) The potential energy profile for the formic acid (FA) and acetic acid (AA) assisted  $\text{H}_2\text{CO}_3 \rightarrow \text{CO}_2 + \text{H}_2\text{O}$  decomposition reactions. (B) The potential energy profile for the sulfuric acid (SA) and hydroperoxide ( $\text{HO}_2$ ) radical assisted  $\text{H}_2\text{CO}_3 \rightarrow \text{CO}_2 + \text{H}_2\text{O}$  decomposition reactions. The energy

profiles have been calculated at the MP2/aug-cc-pVTZ level of theory including zero point vibration energy (ZPE) corrections.

Figure 1:



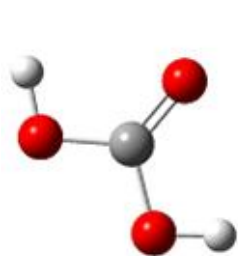
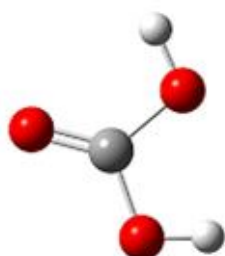
**Figure 2:****(cc)-H<sub>2</sub>CO<sub>3</sub>****(ct)-H<sub>2</sub>CO<sub>3</sub>**

Figure 3:

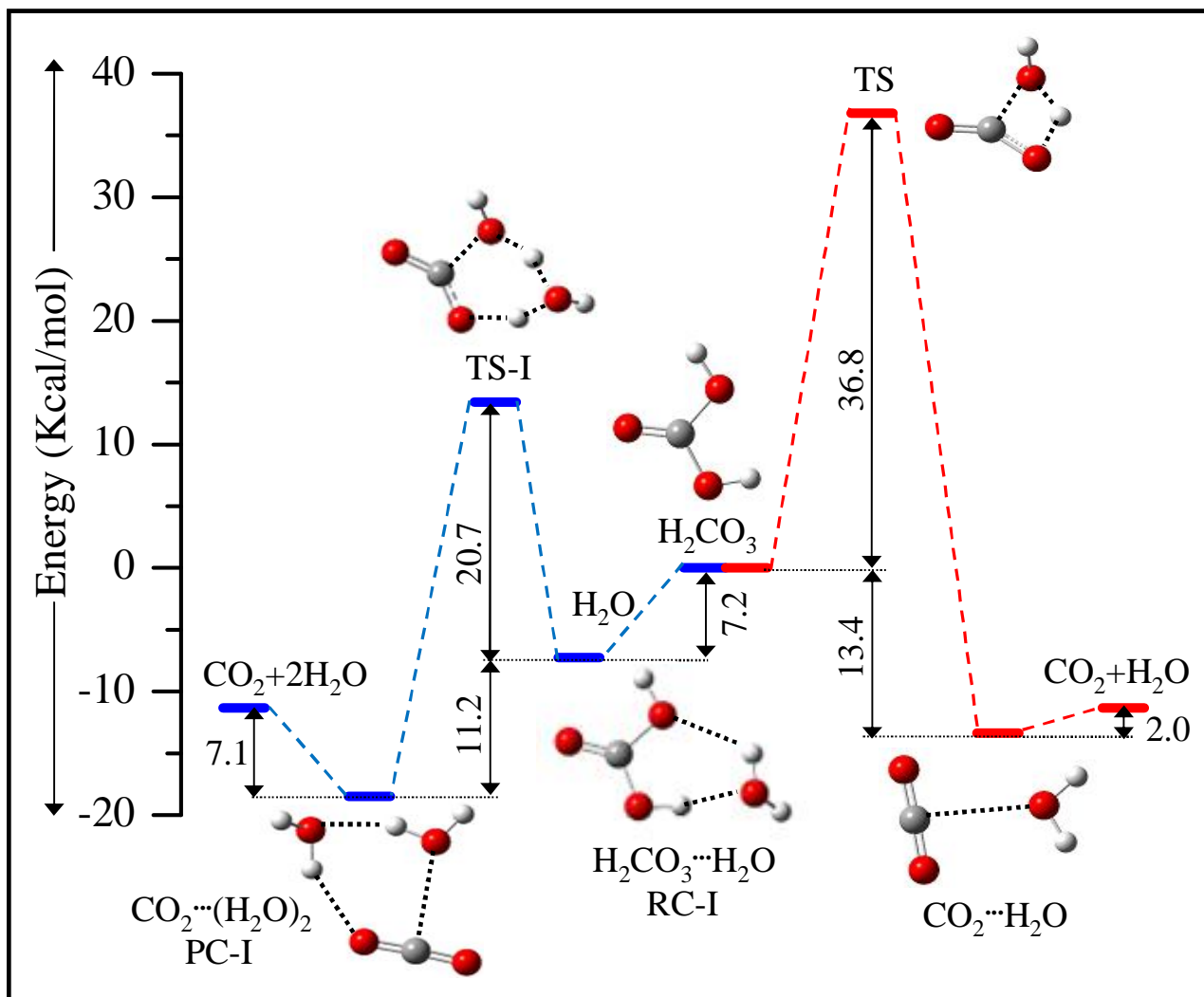


Figure 4:

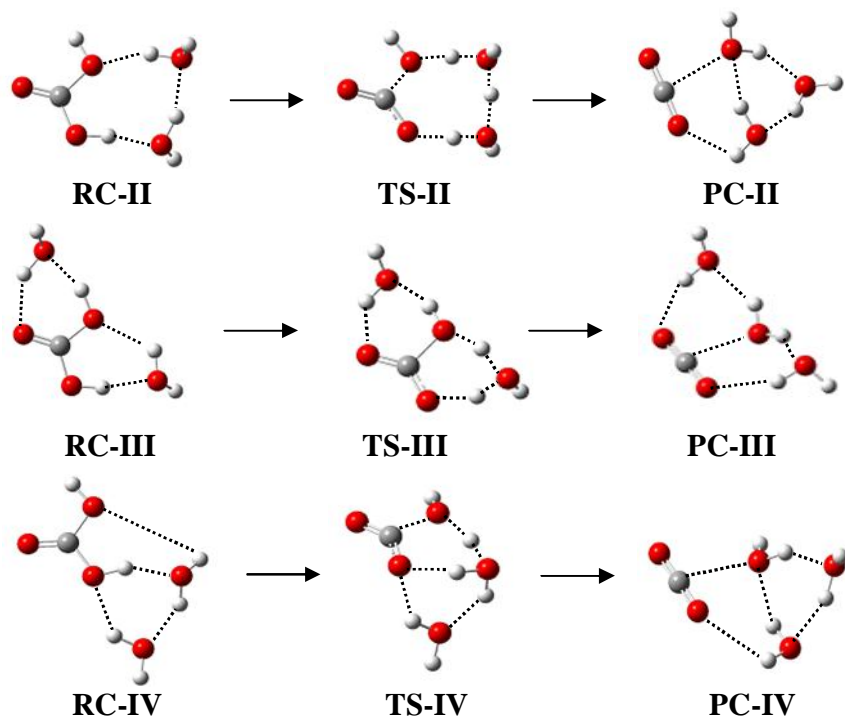


Figure 5:

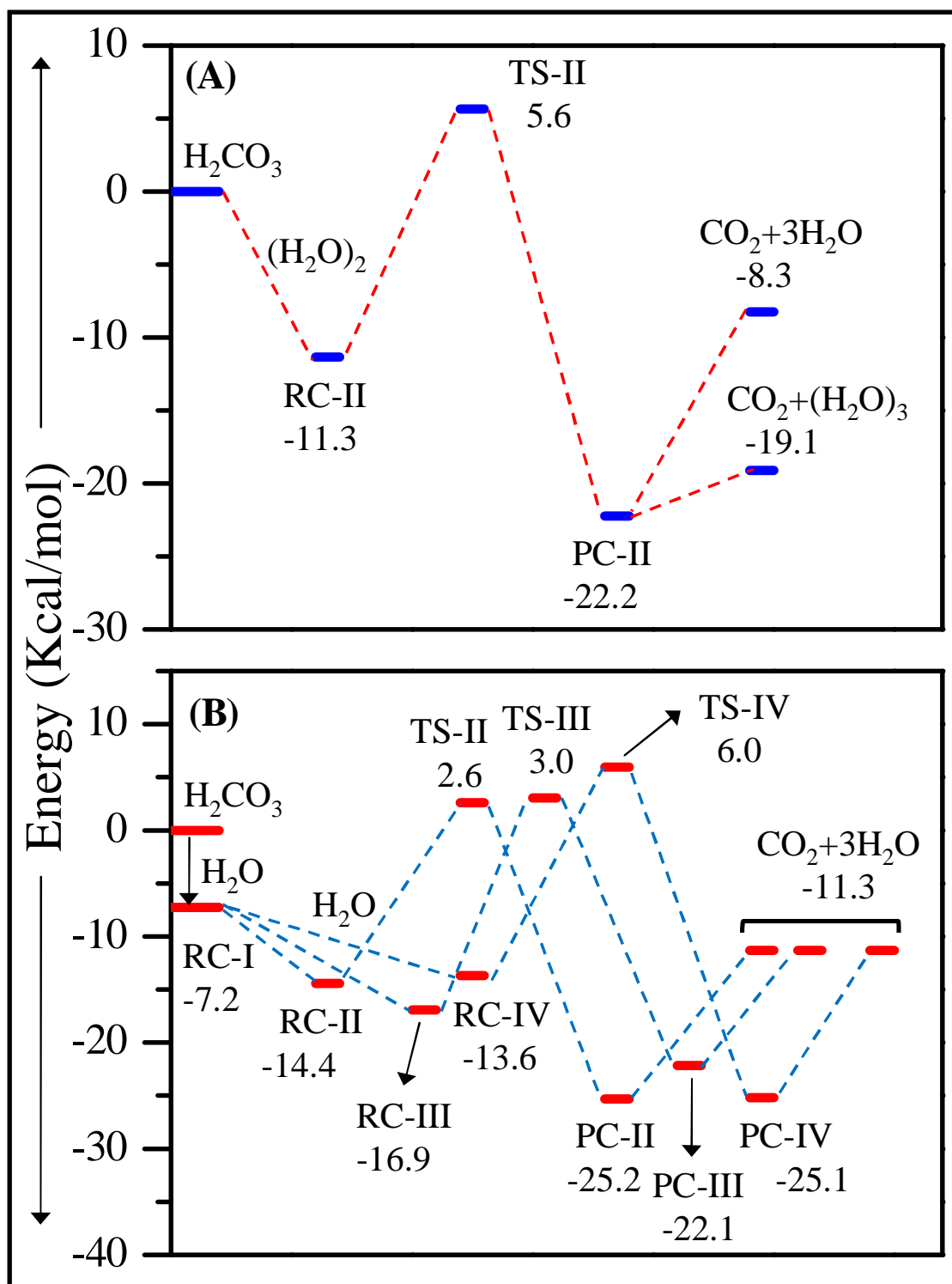


Figure 6:

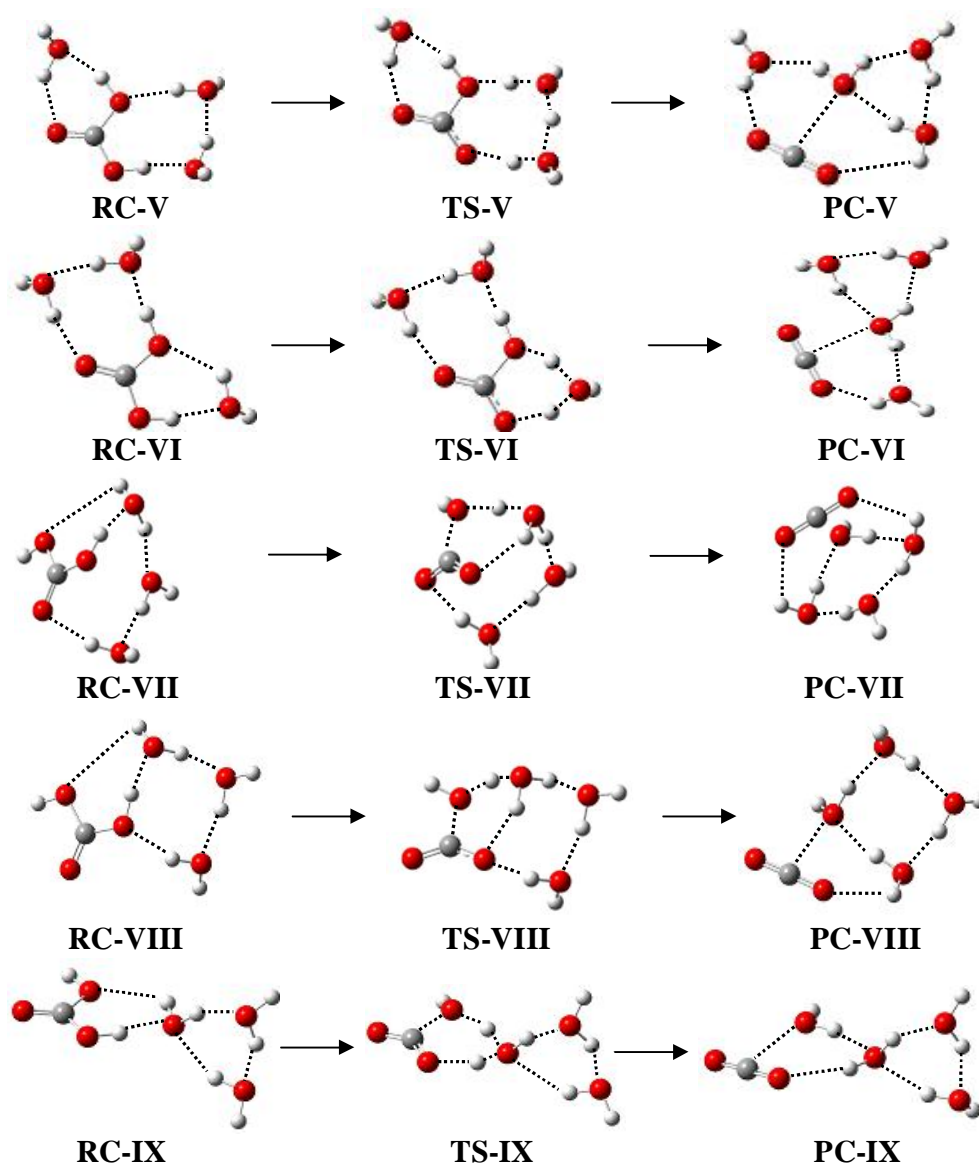


Figure 7:

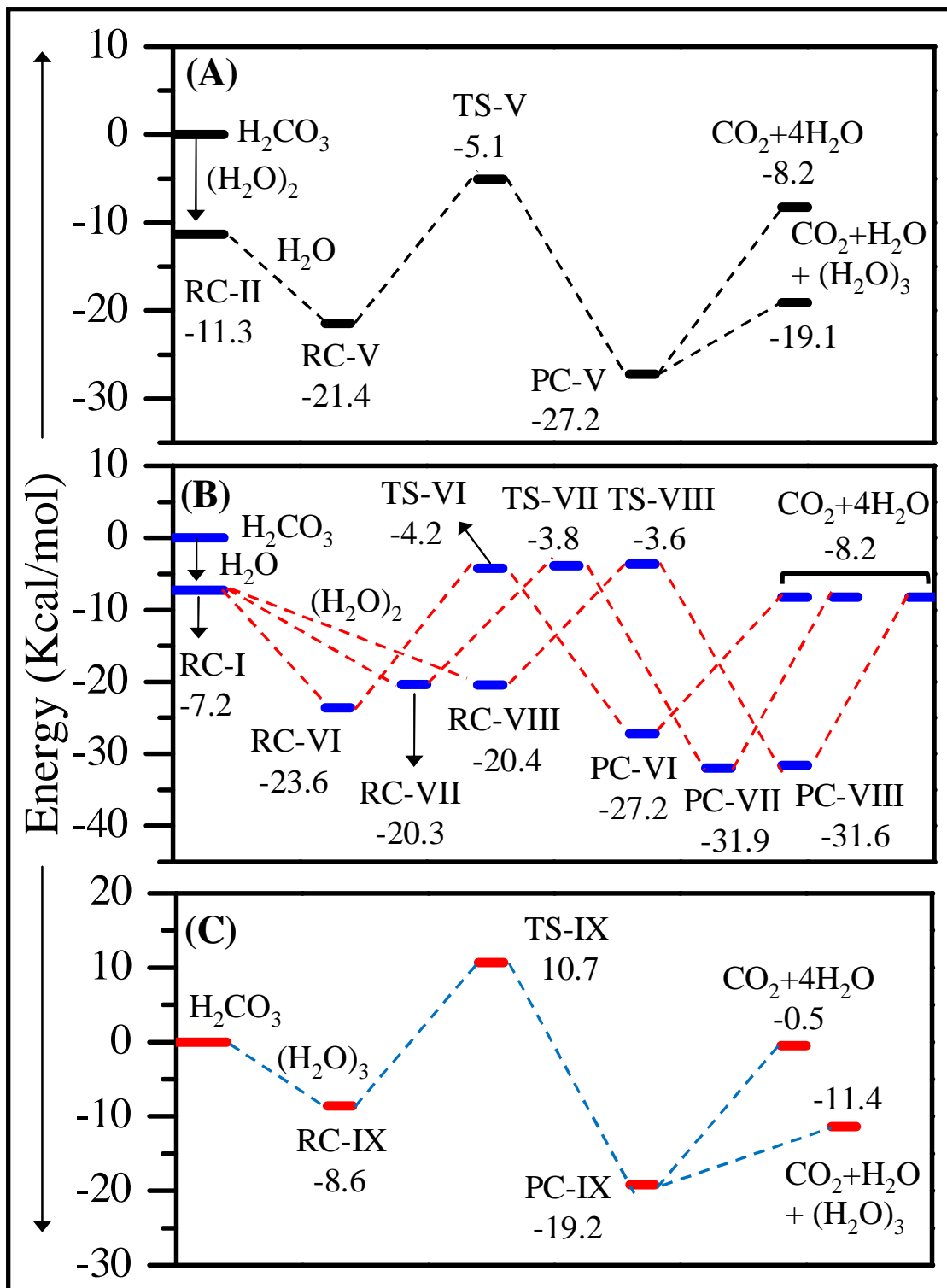


Figure 8:

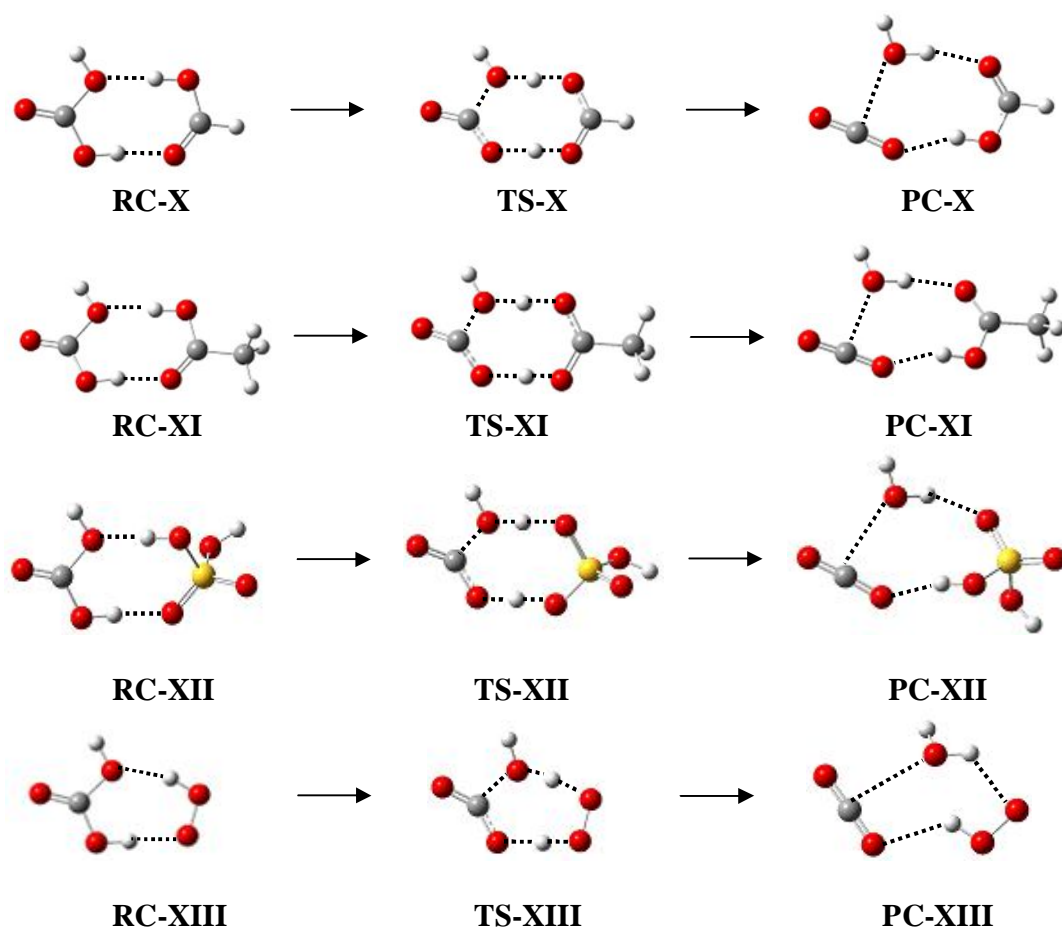
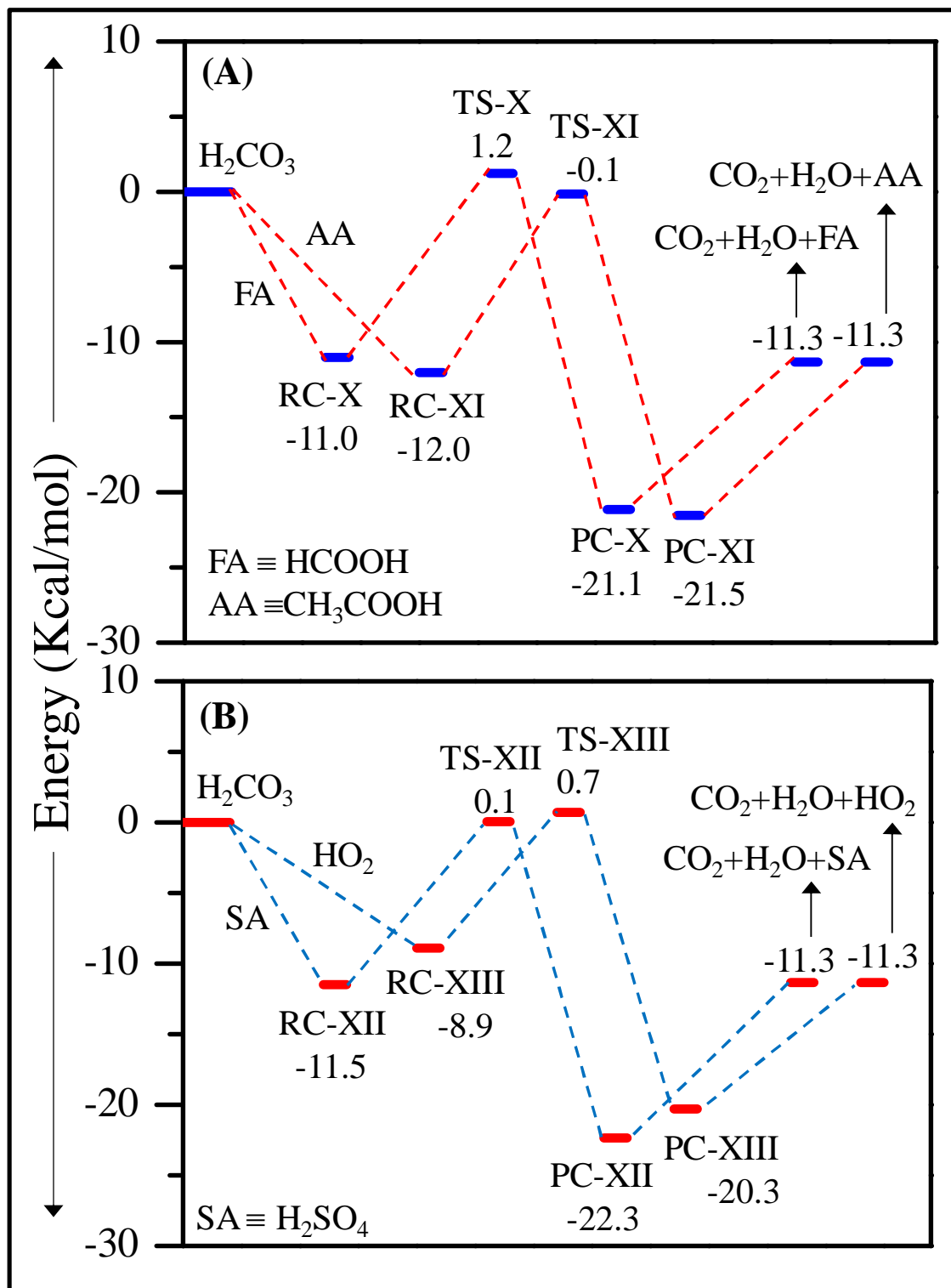
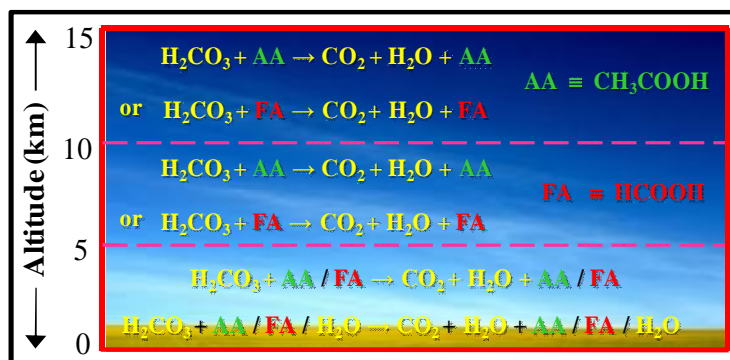


Figure 9:



## Graphical Abstract



Carbonic Acid Decomposition of Potential Atmospheric Significance